Mojave Science Newsletter

Natural Reserve System
UNIVERSITY OF CALIFORNIA

*Promoting science-based field studies throughout the eastern Mojave Desert of California*

# Niche Models Based on Precipitation and Temperature Show Little Climatic Differences Between *Linanthus parryae* Color Morphs

Ioana Anghel[1], Shaan Goel[1], and Felipe Zapata[1]

Some polymorphisms are maintained by natural selection. Within populations, selective forces must be strong enough to overcome gene flow and favor multiple phenotypes (*1*). When polymorphisms exist between populations (i.e., each population displays the alternative state of the polymorphism), the same within population disruptive selective pressures may be acting unidirectionally, leading to one morph or the other surviving in a given location. The forces that maintain the polymorphism locally or between populations may be playing out across the landscape as well, segregating the morphs into populations. If the selective pressure is environmental, locally adapted morphs may diverge over time (*2*). An alternative explanation for color morph distribution is genetic drift, a process by which populations diverge over time because of random mutations and lack of gene flow. With genetic drift, populations that are closer together are more similar, while those separated by greater distances experience less intermixing and are more different (*3*). Though selection and genetic drift are sometimes described as diametric, they both operate to create variation within species to varying extents.

**Figure 1. The two morphs of *Linanthus parryae*, both photos taken at Short Canyon, near Ridgecrest, California. Left photo shows a population of the white morph. The right photo shows a blue morph individual. Photos by Ioana Anghel.**

Understanding the maintenance of petal color polymorphism in *Linanthus parryae* has motivated decades of debate and discovery in population genetics and landscape genomics (*4*). *Linanthus parryae* is an iconic annual Mojave Desert flowering species that can blanket desert washes on years with high relative rainfall. Populations can be monomorphic for petal color with just blue or just white flowered-individuals, or polymorphic with both blue and white-flowered individuals (Fig. 1). Previous research has shown that in a polymorphic population in the Mojave Desert, the two morphs persisted due to rainfall variability (*4, 5*). In rare years when rainfall was relatively high, white-flowered individuals showed higher fitness than blue-flowered individuals, producing significantly more seeds (*4, 5*). Precipitation was low in most years, and the seeds of *L. parryae* either rested in the seed bank, or the blue-flowered morphs had higher relative seed production. Rainfall-driven fluctuating selection may be the mechanism maintaining this flower color polymorphism locally. Yet, it is not known whether these same selective pressures operate at the landscape level maintaining differences across *L. parryae* monomorphic populations.

Here, we investigate whether the climatic differences that may be responsible for selection at the local level in polymorphic populations of *L. parryae* are also operating at the landscape level in monomorphic populations. Do blue monomorphic populations occupy a different climatic niche than white monomorphic populations?

**In this Issue:**



[1] University of California, Los Angeles.

To answer this question, we used ecological niche modeling to understand and forecast the geographic distribution of species based on environmental variables. We obtained occurrence data from the Global Biodiversity Information Facility (GBIF), an international database that aggregates accessible geographical information about species on Earth. GBIF is a widely used resource for biologists, compiling occurrence data from multiple sources including “citizen scientists” and natural history collections. One limitation of using GBIF is spatial bias, because most observations and collections are made near populated or easily accessible areas. This bias may be especially pronounced in desert areas, because people are more likely to visit easily accessible locations along roads and trails.

First, we downloaded *L. parryae* occurrences from GBIF and filtered out records observed before 1970, those without coordinate data, those with coordinate uncertainty greater than 2500 meters, and those that were found outside the species distribution and likely a misidentification (*6*). We then used the record notes, scanned herbarium sheet images, or associated photos to code records for color as either white, blue or polymorphic. To code an occurrence as polymorphic, we looked for both morphs in the photo or herbarium scan, the observation notes, or if two locations with different morphs were within 0.01 degrees of each other in their locality information (corresponding to a maximum of 1.4 km). We considered records within 0.01 degrees of each other that were of the same morph to be duplicates and removed them. We then disregarded the polymorphic populations and divided the data into blue or white flower observations. The input data sets had 71 blue observations and 173 white observations.

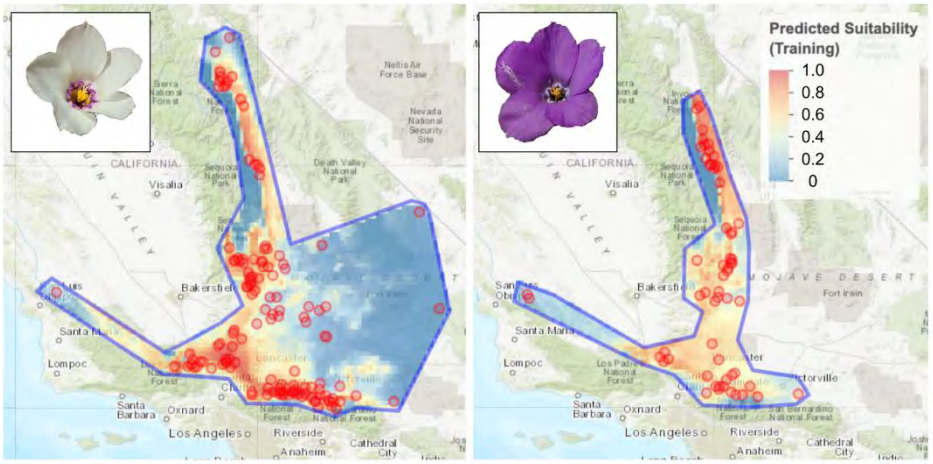


**Figure 2. Geographic prediction of white and blue morphs based on their climatic niches, with observations indicated by red circles. The highest predicted suitability of whites was in the southern Mojave Desert, and the highest suitability of blues was in northern Owens Valley.**

We modeled the ecological niche separately for the two color morphs using the Wallace v2.0.6 (7) workflow. We used the 19 WorldClim environmental variables at a resolution of 2.5 arc minutes, all of which relate to temperature and precipitation patterns recorded between 1970-2000 across the entire globe (*8*). Examples of the variables include annual mean temperature (BIO1), temperature seasonality (BIO4), max temperature of warmest month (BIO5), precipitation of wettest month (BIO13), precipitation of driest month (BIO14), precipitation of driest quarter (BIO17), and precipitation of warmest quarter (BIO18); to see the full list of variables, visit www.worldclim.org/data/bioclim.html. At the latitudes where our samples were sourced from (34 - 38 latitude), 2.5 arc minutes corresponds to 3.6 to 3.8 km. Records occurring in the same environmental grid cell with 0.7 km spatial thinning were filtered, resulting in a total of 59 blue and 132 white-flowered records. After delimiting the geographic range of each morph and sampling environmental background points (1280 and 3200 for the blue and white morphs, respectively), we used a Principal Components Analysis (PCA)[1] to simplify the multidimensional set of environmental variables and more easily identify the patterns in the data. We then created an occurrence density grid in environmental space with PC1 and PC2, and quantified niche overlap using the occurrence grid.

We partitioned the data spatially into four groups in a checkerboard pattern with an aggregation factor of two. We then ran the Maxent[2] algorithm (*9*), estimating an environmental niche model for both morphs. We ran multiple models including combinations of the feature classes (linear, quadratic, or both), with regularization multipliers of 1-5, a step value of one, and clamping, which resulted in 15 models. We chose a model based on the best corrected Akaike Information Criterion (AICc) score[3], which was the model with both linear and quadratic feature classes and a regularization multiplier of two, and visualized predicted habitat suitability. Then, we ran a niche similarity test, which uses a one-tailed test to determine whether the two morphs had more overlap than a simulated set of random niche overlaps.

Overall, we found little differences in the niches of the two morphs. The predicted habitat suitability map showed that the white morph was more concentrated in the southern Mojave Desert at the foothills of the Transverse Ranges, while the blue was more concentrated in northern Owens Valley (Fig. 2). The blues and whites occupied slightly different environmental spaces

(Fig. 3), but the niche similarity test revealed that the niches of the two morphs were more similar to each other than 98% of the null simulated data (p=0.02, Fig. 4). That is to say that the niches of the two morphs were not significantly different.

In the PCA two-dimensional space, the two morphs had little differences in spread, with the blue morph slightly occupying lower values in the PC2 axis (Fig. 2). The climatic variables that have high negative loadings in PC2 and that may be driving the slight blue morph differences were BIO4, BIO14, BIO18, and BIO17 (see above for code translations), associated with temperature seasonality and dry season precipitation. This indicates that the blue morph may occur in regions with lower temperature ranges and lower summer rainfall. The climatic variables with high positive loadings in PC2 were BIO15, precipitation seasonality and BIO3, isothermality. The white morph occupied higher values on the PC2 axis, and the associated variables may indicate that whites occur in areas with higher rainfall fluctuations over the year but more constant temperatures.

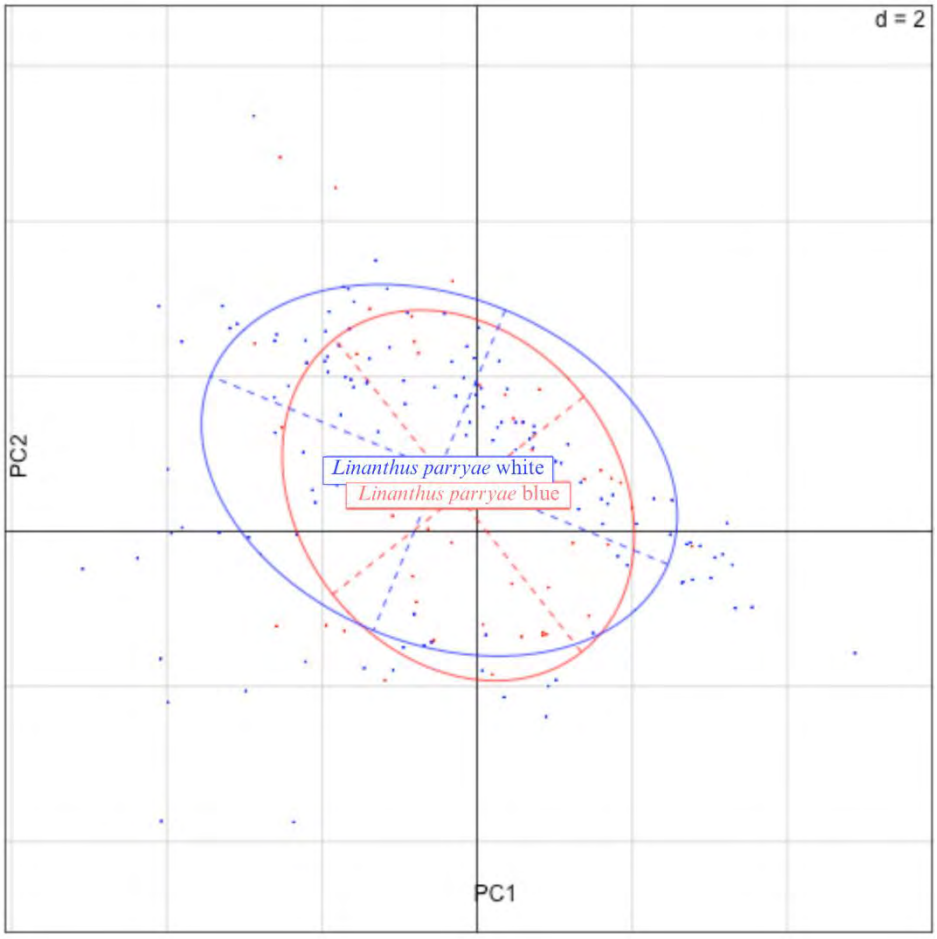


**Figure 3. Principal Component Analysis (PCA) plots each occurrence point with its associated environmental variability depicted in the two largest axes of differentiation. The ellipses depict the climatic variance of each morph, showing the relative positions of the niche of each morph. There is very little differentiation between the two morphs, along with substantial portions of overlap. The PC1 axis explained 65.2% of the climatic variation and the PC2 axis explained 21.7%.**

If the same environmental forces maintaining the polymorphism locally were also operating at the landscape level, we would expect to find niche differences between the blues and whites using our data. We found no significant difference between the two morphs using the niche models built with the WorldClim climatic variables. However, we did find a slight partition of environmental space between the two morphs. Our lack of detection of niche differences may indicate that selection at the landscape level may be obscured by other evolutionary forces, like genetic drift and migration *(10, 11)*. It may also indicate that we did not capture the right set of variables that act as agents of selection. At the local level, it has been shown that the habitat for the two morphs differed in mineral uptake, soil composition and plant community (*5*). Our study did not include these environmental factors, but a future study including these parameters at the landscape level would complement our results.

Whether selection or random change is driving the color morph pattern at the landscape level is difficult to untangle with our data because we only have observations for each location at one point in time. Previous work showed that the polymorphism may be maintained by fluctuating selection mediated by rainfall patterns (*4, 12*), and year to year variability is not captured through the WorldClim variables we used. In addition, some of the populations that we coded as monomorphic may be polymorphic in other unobserved years. Fine-scale multi-year observations are needed to quantify whether a population is truly monomorphic or polymorphic.

We expected environmental variables associated with precipitation to drive the niche differences between the two morphs on a landscape scale, but we did not find a strong association. The slight difference in niches was associated with low dry season precipitation in the blue, and high precipitation seasonality in the white. These climatic differences may indicate that blues are more likely to survive to the flowering stage in areas that have low out of season precipitation. The white morphs are perhaps more likely to survive to the flowering stage in areas where rainfall is most consistent in a certain season, likely the winter.

The environmental variables favoring one morph over the other are likely much more complex on both a spatial and temporal scale than those captured by the WorldClim climatic variables. Identifying the variables that incorporate the desert's inconsistent and variable precipitation year to year as well as more fine scale rainfall measurements will help us better understand the maintenance of the *L. parryae* polymorphism.

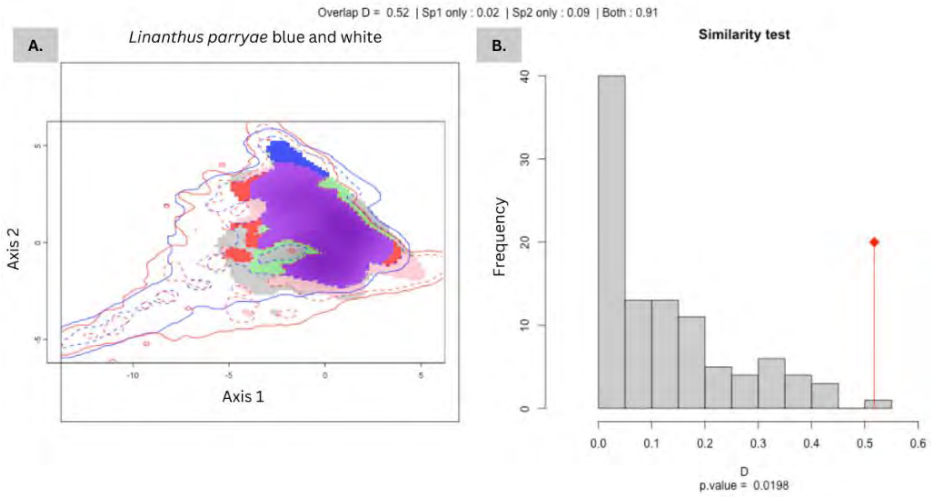


**Figure 4. A. The environmental space occupied by the blue morph is in red and the white in blue. Purple represents the environmental space shared by the two morphs. The gray represents null overlap. Schoener's D metric quantifies niche overlap as the extent to which both morphs are likely to be present at any location (*11*). There was 0.52 niche overlap between the morphs (out of 1.00 maximum), with 0.02 of environmental space occupied by the blue morph only, and 0.09 occupied by the white morph only. B. The similarity test shows that the two morphs were more similar than random, with a 0.02 p-value. This means that the morphs are 98% more similar than a set of random data. The red line indicates the niche overlap quantified by the D metric.**

*Notes*

[1] PCA is a statistical technique that helps simplify multi-dimensional data by quantifying the largest axes of variation in the data. This allows us to visualize the axes that capture the two biggest ranges of variation in the data.

[2] Maxent analysis is a statistical method used to predict where species are likely to be found based on their observed locations and corresponding environmental factors.

[3] AICc is a measure used to compare different statistical models and determine which one best explains the data. Lower AIC scores indicate a better-fitting model.

*References*


1. D. J. Futuyma, *Evolution* (Sinauer Associates, Sunderland, Massachusetts, ed. 3rd, 2013).
2. C. A. Mclean, D. Stuart-Fox, Geographic variation in animal colour polymorphisms and its role in speciation. *Biol. Rev.* **89**, 860–873 (2014).
3. S. Wright, Isolation by distance. *Genetics* **28**(2), 114–138 (1943).
4. D. W. Schemske, P. Bierzychudek, Perspective: Evolution of flower color in the desert annual *Linanthus parryae*: Wright revisited. *Evolution* **55**, 1269–1282 (2001).
5. D. W. Schemske, P. Bierzychudek, Spatial differentiation for flower color in the desert annual *Linanthus parryae*: Was Wright right? *Evolution* **61**, 2528–2543 (2007).
6. GBIF.org (11 October 2024) GBIF Occurrence Download. https://doi.org/10.15468/dl.vvhp5e
7. J. M. Kass, G. E. Pinilla-Buitrago, A. Paz, B. A. Johnson, V. Grisales-Betancur, S. I. Meenan, D. Attali, O. Broennimann, P. J. Galante, B. S. Maitner, H. L. Owens, S. Varela, M. E. Aiello-Lammens, C. Merow, M. E. Blair, R. P. Anderson, Wallace 2: A shiny app for modeling species niches and distributions redesigned to facilitate expansion via module contributions. *Ecography* 1–9 (2023).
8. S. E. Fick, R. J. Hijmans, WorldClim 2: New 1-km spatial resolution climate surfaces for global land areas. *Int. J. Climatol.* **37**, 4302–4315 (2017).
9. D. L. Warren, S. N. Seifert, Ecological niche modeling in Maxent: The importance of model complexity and the performance of model selection criteria. *Ecol. Appl.* **21**, 335–342 (2011).
10. P. R. Reillo, D. H. Wise, An experimental evaluation of selection on color morphs of the polymorphic spider *Enoplognatha ovata* (Araneae: Theridiidae). *Evolution* **42**, 1172–1189 (1988).
11. T. W. Schoener, The Anolis lizards of Bimini: Resource partitioning in a complex fauna. *Ecology* **49**, 704–726 (1968).
12. M. Turelli, D. W. Schemske, P. Bierzychudek, Stable two-allele polymorphisms maintained by fluctuating fitnesses and seed banks: Protecting the blues in *Linanthus parryae*. *Evolution* **55**, 1283–1298 (2001).

# Documenting California's Insect Diversity: A Two-Year Deluge of Species Barcodes

Julia Perez[1], Jacob Jones[1], John Heraty[1], and Christiane Weirauch[1]

Systematists document and describe the vast diversity of plants and animals living on the planet, and as such, their research is one of the essential foundations of all biological science. This task becomes even more challenging and urgent as our world changes rapidly around us. Our natural landscapes are being degraded or destroyed at an accelerating pace for the sake of land development, agriculture, and other activities of the burgeoning human population (*1*). The increased use of commercial pesticides has particularly impacted insect numbers and their habitats (*2*). California is the home of a biodiversity hotspot, the California Floristic Province, while also serving as an agricultural powerhouse for the rest of the country. Many efforts are underway to support the conservation and long-term protection of California's biodiversity and habitats. One such effort is Executive Order N-82-20 (*3*), which commissioned the California Insect Barcoding Initiative (CIBI) to database genetic identification of every insect species in California. One goal of this initiative is to "Establish a baseline assessment of California's biodiversity that builds upon existing data and information, utilizes best available science and traditional ecological knowledge, that can be updated over time" (*3*). We have made strides to reach these goals with funding generously awarded by the State of California to the California Institute for Biodiversity, which is supporting a collaborative effort of seven different academic organizations to conduct the necessary research to achieve those goals; the seven organizations include: California Academy of Sciences, California Department of Food and Agriculture, Natural History Museum of Los Angeles, San Diego Natural History Museum, UC Berkeley, UC Davis, and UC Riverside. We present in this paper a current overview of the data collected by our group, led by Dr. John Heraty and Dr. Christiane Weirauch, at UC Riverside.

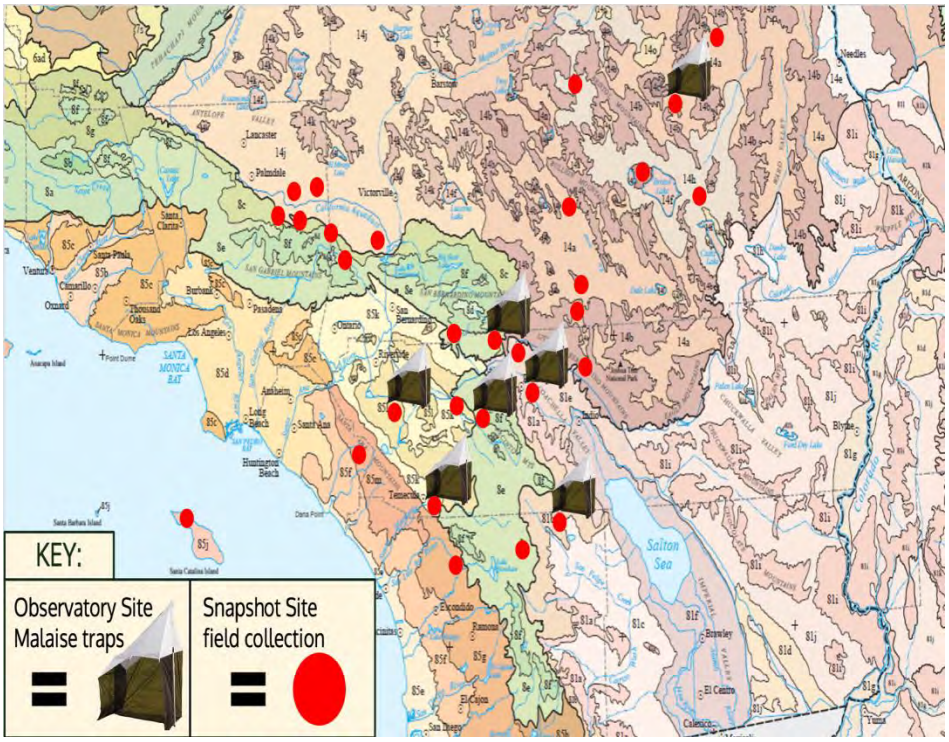


**Figure 1. Section of the ecoregion map published by Griffith et. al. (2016) focusing on Southern California. Shown are the localities of the seven Malaise traps placed by the UCR team for passive collection from March through October of 2023 along with the Snapshot Sites in the surrounding areas.**

Through our CIBI grant, we are collecting and digitally databasing Californian insects in order to more accurately catalog the species we have. We are accomplishing this by collecting physical specimens of as many insect species in the wild as possible, then assigning a genetic identification label or 'DNA barcode' for each unique specimen. Identifying all the specimens using dichotomous keys would be too time consuming, so instead we are developing a reference library of sequenced DNA that is used to produce the DNA barcodes using a portion of the mitochondrial gene, cytochrome c oxidase subunit I (CO1). This gene has been considered reliable in insects and other invertebrates for distinguishing species based on their genetic distance, which is assumed to be greater for species that do not interbreed because each distinct taxon will accumulate species-specific differences in their maternally inherited mitochondrial loci (*4*). Insect specimens are being submitted through the Natural History Museum of Los Angeles County to the Center for Biodiversity Genomics at the University of Guelph. The Canadian Centre for DNA Barcoding was founded in 2006 and is now the largest contributor of sequences to the global repository of DNA barcodes, the Barcode of Life Data (BOLD) System. At Guelph, specimens are separated, then photographed before their DNA is extracted and a fragment of CO1 is amplified by PCR to produce a detectable genetic signal for assessment. To better understand the

[1] University of California Riverside.

massive amounts of DNA data being processed, similar specimen barcodes are clustered into Barcode Index Numbers (BINs) and species are sorted by the degree of genetic divergence between BINs (typically >3%) (*5*). If a species name has been applied to a BIN based on previous work, then a matching BIN can also be identified to that species name; but if not, that BIN may represent one of the many undescribed species in California, or a described species that has yet to be CO1 sequenced. Any BINs that do not match something already in the database are given a unique BIN for Guelph's barcode library and are flagged for further analysis. One major outcome of producing this genetic library of California insects is that researchers can prioritize the unique BINs, which are likely to be discrete species, for focused sample collecting as a means to publish new species descriptions in the future. Another outcome of this research is that new geographic distributions for known taxa (with previously documented BINs) will serve as important data to help ecologists track changing distributions of insect species across the West Coast, for example, due to climate change. DNA barcoding is still a relatively new form of insect documentation, so our libraries are nowhere near completion. Fortunately, it is now possible for CIBI to document BINs that represent the many thousands of currently known species that have yet to be added to the DNA library in a standardized and widely accessible data format.

As this project was estimated to take place over the course of only two years, we had to take a methodical approach to streamline our techniques and maximize the number of insects to be barcoded from within such a large boundary. California is home to a unique and variable landscape that comprises sweeping diversity of different ecosystems and habitats. These unique ecological regions or 'ecoregions' are defined as "areas of general similarity in ecosystems and in the type, quality, and quantity of environmental resources" and are a way to distinguish regions on a map that are relatively similar to one another (*6*). For the purposes of the UCR CIBI project we used the level III and IV ecoregions defined by USGS in 2016 (*6*), where the latter category divides California into 177 ecoregions within 13 level III ecoregions. The thirteen sections span across the state, allowing each of our institutions to divvy up and thoroughly sample specific wildlands in our respective proximity. Upon considering these level III ecoregions, we established 50 locations where one of the seven institutions would run 'Observatory Site' sampling via Malaise trapping. Additionally, each institution added 'Snapshot Sites', which are individual collection events, to fill in any perceived geographical or ecological gaps in the overall sampling effort. At UC Riverside, we were responsible for seven of the 50 Observatory Sites in California. Six of these seven localities are situated at UC Natural Reserve System field stations, including: Boyd Deep Canyon Desert Research Center (Piñon Flats), Motte Rimrock Reserve, Emerson Oaks Reserve, James San Jacinto Mountains Reserve, Oasis de Los Osos Reserve, and Sweeney Granite Mountains Desert Research Center (Fig. 1). In addition to these six reserves, we also had an Observatory Site at Whitewater Preserve. The UC reserves we selected encompass four of California's 13 level III ecoregions (Table 1), allowing us to collect insects from diverse ecosystems with Malaise traps in 2023.

A Malaise trap is a collection tool that passively captures insects using flight interception and naturally directs them into the top of a tent-like peak which opens to a chamber connected to a 500 mL bottle full of ethanol or propylene glycol (Fig. 2) (*7*). These traps work exceptionally well for collecting Diptera (flies), Hymenoptera (ants, bees, and wasps), and Lepidoptera (butterflies and moths), but are more limited in collecting other notable orders of insects such as Coleoptera (beetles) and Hemiptera (true bugs) (*8*). The 50 Observatory Sites across all institutions were selected to provide us with uniform sampling across as many of California's ecoregions as possible, from the months of March through October, typically when

**Figure 2. Malaise trap location for our Sweeney Granite Mountains Desert Research Center Observatory Site. This passive collection trap sat nestled in Granite Cove facing west to maximize insect collection.**

insects are most active. The Malaise traps were open for the first week of each month, after which, the bottle was removed and the trap left inactive for the remainder of the month to limit over-collecting. During peak season, these bottles were often brimming with such an abundance of insects that the contents of the bottle became an opaque agglomeration, which we dubbed 'black gold' due to the potentially rich insect biodiversity captured within. These unsorted Malaise samples were sent to Guelph for sequencing, with the end goal of having standardized data sets for future biodiversity analyses. Another outcome of collecting in this way was to potentially include cryptic taxa that have never been documented.

Malaise sampling alone is not the best method to maximize species richness measures or to get a complete survey of California insects because many groups of terrestrial or aquatic insects must be collected using different methods. Insects can occupy very specific niches that can be difficult to find and document. To account for gaps in our Observatory Site data, we

also collected insects at 'Snapshot Sites' within the state to help bridge the gaps in our Observatory Site (Malaise trap) sampling. The main goal was to establish Snapshot Site localities within unsampled ecoregions. These collection events are not limited to Malaise trapping but include a plethora of other insect collecting techniques. We prioritized sweep netting, where we sweep an insect net across tall grasses, shrubs and trees within reach. In addition, we frequently utilized aquatic nets and dip nets for aquatic insect collection, as well as drag nets for terrestrial insects. We also deployed bait traps, pan traps, and light traps overnight (using mercury vapor and ultraviolet bulbs) (Figs. 3 and 4). The benefit of using more passive collection methods, such as light traps, is that they allow us to wait for insects to come to us! The light bulb draws insects toward it because the bulb emits UV light that insects mistake for the moon, which they use to orient themselves (*9*). Using these various collection methods, we were able to collect a larger diversity of insects than those frequently encountered in Malaise traps.

**Table 1. Locality and ecoregion information of each Observatory Site sampled by UCR. Organized by the sequential order in which we visited localities and colorized to their respective level III ecoregion as per the Environmental Protection Agency's ecoregion map palette.**

| Observatory Site | Latitude | Longitude | Elevation (m) | Level III Ecoregion | Level IV Ecoregion | Characteristic Plants |
|---|---|---|---|---|---|---|
| Motte Rimrock Reserve | 33.8051 | -117.2598 | 557 | 85 | Inland Hills | Sage scrub and perennial grasses |
| Emerson Oaks Reserve | 33.4657 | -117.0412 | 478 | 85 | Inland Valleys | Oak and coastal sage scrub |
| Boyd Deep Canyon Desert Research Center (Piñon Flats) | 33.6057 | -116.4506 | 1299 | 81 | Western Sonoran Mountain Woodland and Shrubland | Juniper and desert scrub |
| James San Jacinto Mountains Reserve | 33.8096 | -116.7783 | 1674 | 8 | Southern California Montane Conifer Forest | Juniper and Conifer Forest |
| Whitewater Preserve | 33.9871 | -116.6553 | 665 | 8 | Arid Montane Slopes | *Encelia* and riparian grasses |
| Oasis de Los Osos Reserve | 33.8894 | -116.6864 | 404 | 81 | Upper Coachella Valley and Hills | Semi-desert shrub and cacti |
| Sweeney Granite Mountains Desert Research Center | 34.7828 | -115.6508 | 1293 | 14 | Eastern Mojave Low Ranges and Arid Footslopes | Creosote, *Yucca*, and *Acacia* |

**Figure 3. A typical light trap set up for night collection. Two large white bed sheets are laid on the ground held down by rocks from the surrounding area. These sheets help illuminate the surrounding night sky by reflecting the mercury vapor bulb above them. This light trap has just been set up, so there are not many insects around it, however in a matter of only minutes, it can quickly change to a swarm of insects from all around.**

The unusually wet winter season from 2022 to 2023 both helped and harmed our cause. As a result of the rain, we experienced California's famed and sporadic 'superbloom' the following spring of 2023. This created an extraordinary surge of pollen, nectar, and greenery which in turn encouraged insect populations to grow (*10*). However, the heavy rains hampered our ability to collect insects as it stayed cooler for longer, delaying the collection season to late March. The weather also created logistical problems in getting the traps set up at two of our sites (Sweeney Granite Mountains Desert Research Center (GMDRC) and James San Jacinto Mountains Reserve). As expected, however, the abundance of insects can be tracked throughout the season based on precipitation patterns. As an example, the GMDRC experiences a bimodal precipitation pattern, with approximately 25% of the average annual precipitation falling between July-September, and the winter rains, December-March, making up the rest (Fig. 5). Based on the data we collected in 2023, the insect abundance tracks this bimodal pattern very well. Notably, in August the GMDRC received a historic 4.61 inches of rain within 12 hours from Hurricane Hilary. For context, consider that the highest precipitation total for the month of August from 1986 to 2022 is 2.5 inches, with a median value of 0.44 inches. We speculate that the hurricane event caused a significant increase in insect density the following September (Figs. 6 and 7). Unfortunately, we don't know how different this spike was from what might be expected after an "average" summer monsoon season.

As of November 2024, across all projects, we had 910,015 insect specimens documented in the BOLD System. Of these, 88% (633,667 from Observatory Sites and 169,909 from Snapshot collecting) have successfully been sequenced and have been grouped into 35,121 BINs which we presume to be unique species. Across all of the Observatory Sites sampled by UCR, the GMDRC had the greatest wet-weight body mass of specimens collected in Malaise traps in 2023 (Fig. 6). Using all collection methods, we have sampled 3,572 unique BINs from the GMDRC, with 2,779 BINs sampled in 2023 alone, and no sign of a species accumulation plateau (Fig. 7). The majority of specimens sampled at GMDRC in 2023 were Diptera, with the other major groups being Lepidoptera and

Hymenoptera (Fig. 8). Our current specimen count across all projects places us just under our goal of one million individuals. While it may seem counterintuitive to collect and kill these insects for the sake of learning about them, it is important to consider that their DNA will contribute to building a library that will be used for years to come: this data will be a key counterpart to the pinned and preserved insects in museums around the world. Without the sequences from freshly collected specimens processed by Guelph, we would not have barcodes of insects currently in California; conversely, without the barcodes of identified museum specimens, we would not have names to assign to the unique BINs. Insects documented on BOLD Systems receive a voucher image that can be accessed to visually associate a specimen with its museum counterpart. Having both the physical specimen and the DNA sequence is especially advantageous because it allows researchers outside of CIBI to examine physical specimens with a barcode label pinned to it, which links them via QR code to digitized barcode data. Thanks to recent advances in metabarcoding, the mixed contents from a sample bottle of a Malaise trap can be used to identify almost all the insects that were in that sample, thus greatly speeding up the process of comparing samples over time and space (*11*).

It is expected that climate changes causing extreme fluctuations in temperatures and precipitation patterns will affect our natural world, plants and animals. For example, the distribution of the western Joshua tree (*Yucca brevifolia*) is expected to shrink in the southern and lower elevations of its current distribution due, in part, to an increase in extreme high temperature events (*12*). Another example is the predicted habitat expansion, largely due to increased mean annual temperatures, of several mosquito species (*Aedes* and *Culex*) over the next 70 years, impacting more communities and putting people at higher risk for infection by mosquito borne viruses (*13*). The circumstances affecting these taxa could also be why other organisms are projected to shift in geographical distribution over the coming decades. Herein lies the importance of our project. Although the notion of discovering new species of insects is an exciting and important part of this effort, another valuable outcome will be documenting future shifts in distribution for a variety of insects. The environment we live in now is not the same one we will exist in even a decade from now. It's crucial we spend time

**Figure 4. A grouping of pan traps set up at the Sweeney Granite Mountains Desert Research Center. These bowls typically attract pollinator insects that think they are flowers. Each bowl is filled with soapy water which causes insects to sink. Bowls are collected by pouring the soapy water through a net and transferred into a fresh vial where ethanol is added to preserve the insects.**

**Figure 5. Taken at sunset at the Sweeney Granite Mountains Desert Research Center in July 2023. The landscape is still alive, even throughout the summer. Pictured above are several plants such as *Yucca* and *Larrea* which are still green.**

documenting the insects of California before irreversible changes are made to our natural environment, as it will certainly impact us, as well as the wildlife we coexist with.

On another note, one fortunate, and slightly peripheral, outcome of the CIBI project being hosted at UCR was that we were able to bring on two undergraduates to assist us through UCR's NRS Experiential Internship, which is a summer internship offered to provide field-based experiences to students attending local universities (including community colleges). Savannah Horton and Diego Castañeda each spent a summer with us focusing on ants of the Granite Mountains with the goal of updating the list of documented species in the area (Figs. 9 and 10). These ants, of course, were a part of the CIBI project for DNA barcoding, as well. As a result of Savannah's effort, we may have added three new ant species to the list of ants at the Granite Mountains; whereas Diego's preliminary data on abundance of the desert ant, *Pheidole desertorum*, indicates a dramatic decline in numbers when compared to studies from 1998 by another undergraduate, Elizabeth Fessler. Making efforts to collect something as small and innumerable as ants conveys the difficulty and depth of this project and further highlights how even seemingly conspicuous taxa, like ants, have not been documented fully. There is great unknown diversity hidden right before our very eyes.

Changes in animal abundance and diversity across the world are impending and unpredictable. Insects are the most populous group of animals in the world and play an integral role as the primary consumers of the trophic pyramid. All larger consumers are directly dependent on them for survival, whether it be for direct consumption or for pollination of resources. Having named BINs of past and present insect species will allow us to record and better understand changes in the ecosystems around us. A 2022 Biodiversity Fact Sheet released by the California Natural Resources Agency estimated the number of insect species at >30,000 (*14*);

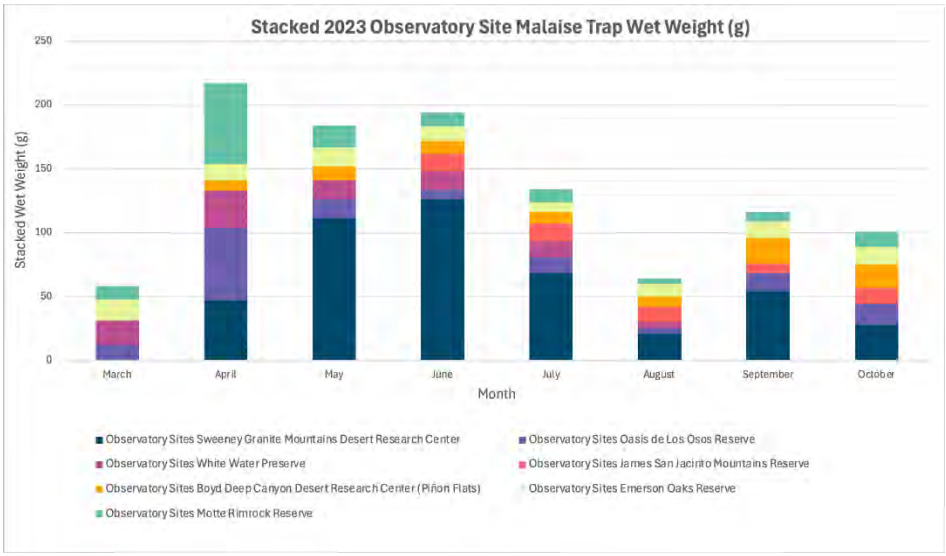


**Figure 6. Monthly wet weight stacked in grams for each Observatory Site over the 2023 collection season. Wet weight is the total mass of all insects captured and measured after being removed from our Malaise trap bottles (but while insects were still wet with ethanol). Boyd Deep Canyon Desert Research Center (Piñon Flats), Sweeney Granite Mountains Desert Research Center, and James San Jacinto Mountains Reserve are missing data for March due to snow, with the latter also missing data in April and May. Whitewater Preserve is missing data in September and October due to roads being washed out from Hurricane Hilary.**

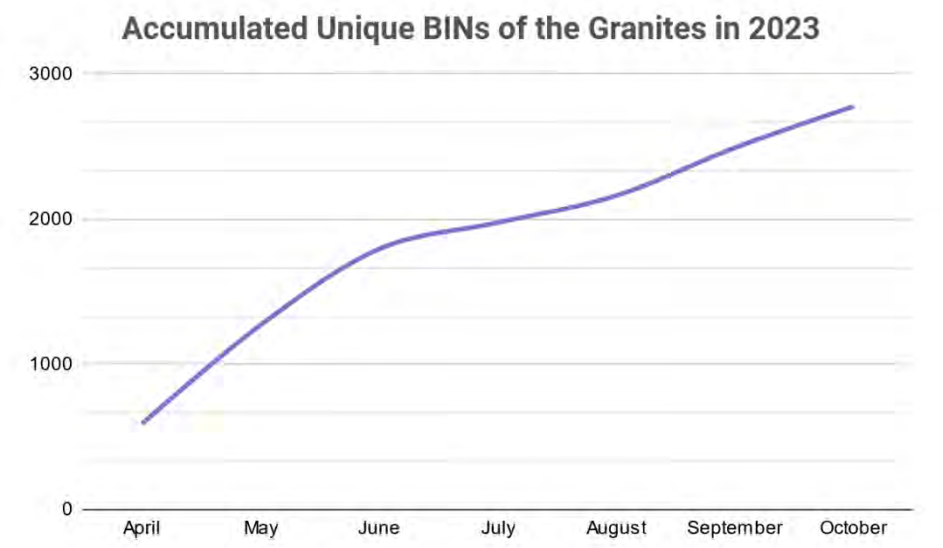


**Figure 7. Line graph representing the accumulated unique BINs at the Granite Mountains in 2023 through various collection methods (Malaise trap, sweep net, light trap, pan trap). Notably the number of new BINs continues to increase suggesting that many new species remain to be discovered.**

however, our current total number of CIBI BINs is already at 35,121 and climbing, suggesting that much of California's biodiversity has historically gone undetected and far underestimated. Comparisons of identified BINs to the known number of species in some groups demonstrates that we are still grossly underestimating the number of species in California. DNA barcoding has now become more accessible than ever before, allowing us to document thousands of undescribed insects in a record amount of time. For this reason, it is important for scientists to embrace new technology that allows us to push the bounds of what we think we already know.

*Acknowledgements*
We would like to thank the generous support of the California Institute for Biodiversity. We also acknowledge the participation of undergraduate NRS student interns, Savannah Horton and Diego

Castañeda, as well as the magnanimous support of the NRS directors in helping with our research.

*References*


1. D. L. Wagner, E. M. Grames, M. L. Forister, M. R. Berenbaum, D. Stopak, Insect decline in the Anthropocene: Death by a thousand cuts. *Proceedings of the National Academy of Sciences* **118**, e2023989118 (2021); https://www.pnas.org/doi/abs/10.1073/pnas.2023989118.
2. M. R. Douglas, D. B. Sponsler, E. V. Lonsdorf, C. M. Grozinger, County-level analysis reveals a rapidly shifting landscape of insecticide hazard to honey bees (Apis mellifera) on US farmland. *Scientific Reports* **10**, 797 (2020); https://www.nature.com/articles/s41598-019-57225-w.
3. Exec. Order N-82-20, SB 337 (2020); https://www.library.ca.gov/wp-content/uploads/GovernmentPublications/executive-order-proclamation/40-N-82-20.pdf.
4. P. D. N. Hebert, A. Cywinska, S. L. Ball, J. R. deWaard, Biological identifications through DNA barcodes. *Proceedings of the Royal Society B* **270**, 313-321 (2003); https://royalsocietypublishing.org/doi/abs/10.1098/rspb.2002.2218.
5. S. Ratnasingham, P. D. N. Hebert, A DNA-Based registry for all animal species: The Barcode Index Number (BIN) System. *PLoS One* **8**, e66213 (2013); https://www.ncbi.nlm.nih.gov/pmc/articles/PMC3704603/.
6. G. E. Griffith, J. M. Omernik, D. W. Smith, T. D. Cook, E. Tallyn, L. Moseley, C. B. Johnson, "Ecoregions of California" (Open-File Report 2016-1021, U.S. Geological Survey, 2016); https://pubs.usgs.gov/publication/ofr20161021.
7. H. Townes, A light-weight Malaise trap. *Entomological News* **83**, 239–247 (1972); https://biostor.org/reference/254324.
8. J. Uhler, P. Haase, L. Hoffmann, T. Hothorn, J. Schmidl, S. Stoll, E. A. R. Welti, J. Buse, J. Müller, A comparison of different Malaise trap types. *Insect Conservation and Diversity* **15**, 666-672 (2022); https://resjournals.onlinelibrary.wiley.com/doi/full/10.1111/icad.12604.
9. S. T. Fabian, Y. Sondhi, P. E. Allen, J. C. Theobald, H. Lin, Why flying insects gather at artificial light. *Nature Communications* **15**, 689 (2024); https://www.nature.com/articles/s41467-024-44785-3.
10. D. L. Denlinger, Seasonal and annual variation of insect abundance in the Nairobi National Park, Kenya. *Biotropica* **12**, 100-106 (1980); https://www.jstor.org/stable/2387725?seq=2.
11. E. Iwaszkiewicz-Eggebrecht, E. Granqvist, M. Buczek, M. Prus, J. Kudlick, T. Roslin, A. J. M. Tack, A. F. Andersson, A. Miraldo, F. Ronquist, P. Łukasik, Optimizing insect metabarcoding using replicated mock communities. *Methods in Ecology and Evolution* **14**, 1130–1146 (2023); https://besjournals.onlinelibrary.wiley.com/doi/full/10.1111/2041-210X.14073.
12. K. L. Cole, K. Ironside, J. Eischeid, G. Garfin, P. B. Duffy, C. Toney, Past and ongoing shifts in Joshua tree distribution support future modeled range contraction. *Ecological Applications* **21**, 137-149 (2011); https://www.fs.usda.gov/rm/pubs_other/rmrs_2011_cole_k001.pdf.
13. M. E. Gorris, A. W. Bartlow, T. Pitts, C. A. Manore, Projections of Aedes and Culex mosquitoes across North and South America in response to climate change. *The Journal of Climate Change and Health* **17**, 100317 (2024); https://www.sciencedirect.com/science/article/pii/S2667278224000208#:~:text=Future%20climate%20and%20land%20use,may%20respond%20differently%20%5B18%5D.
14. California Natural Resources Agency, 2022 Biodiversity Fact Sheet; https://www.google.com/search?client=firefox-b-1-d&q=california+biodiversity+fact+sheet.


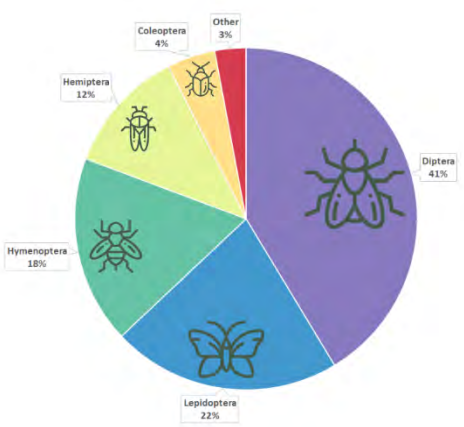


**Figure 8. Pie chart representing proportions of insect orders collected in the Granite Mountains through various collection methods (Malaise trap, sweep net, light trap, pan trap) in 2023.**


**Figure 9. NRS summer intern Diego Castañeda on his first visit to the Granite Mountains Desert Research Center in June 2024.**

**Figure 10. NRS summer intern Savannah Horton collecting ant specimens at 9:00pm in July 2023 when the ants were especially active as temperatures had dropped to 91° after nightfall.**

# The 2023 York Fire, Mojave National Preserve – A Wildfire History Perspective

Joseph R. McAuliffe[1] and James M. André[2]

The York Fire of July to August 2023 was the largest wildfire ever recorded in Mojave National Preserve (Preserve), a unit of the National Park Service since 1994. At the end of the fire's first day on 28 July, the human-ignited blaze was limited to 2,500 acres (10 km$^2$), near the area of ignition in the eastern portion of Pinto Valley and northward into Caruthers Canyon. However, during the second and third days, strong winds rapidly carried the fire more than 20 km to the northeast into neighboring Clark County Nevada, and 10 km to the southeast, increasing the total area 25-fold to over 68,000 acres (275 km$^2$). The fire eventually burned 93,078 acres (377 km$^2$), with a footprint approximately 40 km long and up to 15 km wide in some places. Prior to the York Fire, the June 2005 Hackberry Complex fires, ignited by lightning, burned the largest area recorded in the Preserve (70,736 acres = 286 km$^2$), followed by the July, 2020 Dome Fire, also ignited by lightning, which burned 43,273 acres (175 km$^2$). Before 2005, the June 1994 Lanfair Fire, which burned 9,497 acres (38 km$^2$), was the largest historically recorded wildfire in the Preserve (and its forerunner, the East Mojave National Scenic Area, established in 1980 and administered by the BLM until 1994). Collectively, within the last two decades, the three largest recorded fires have burned approximately 15% of the entire land area of the Preserve (Fig. 1).

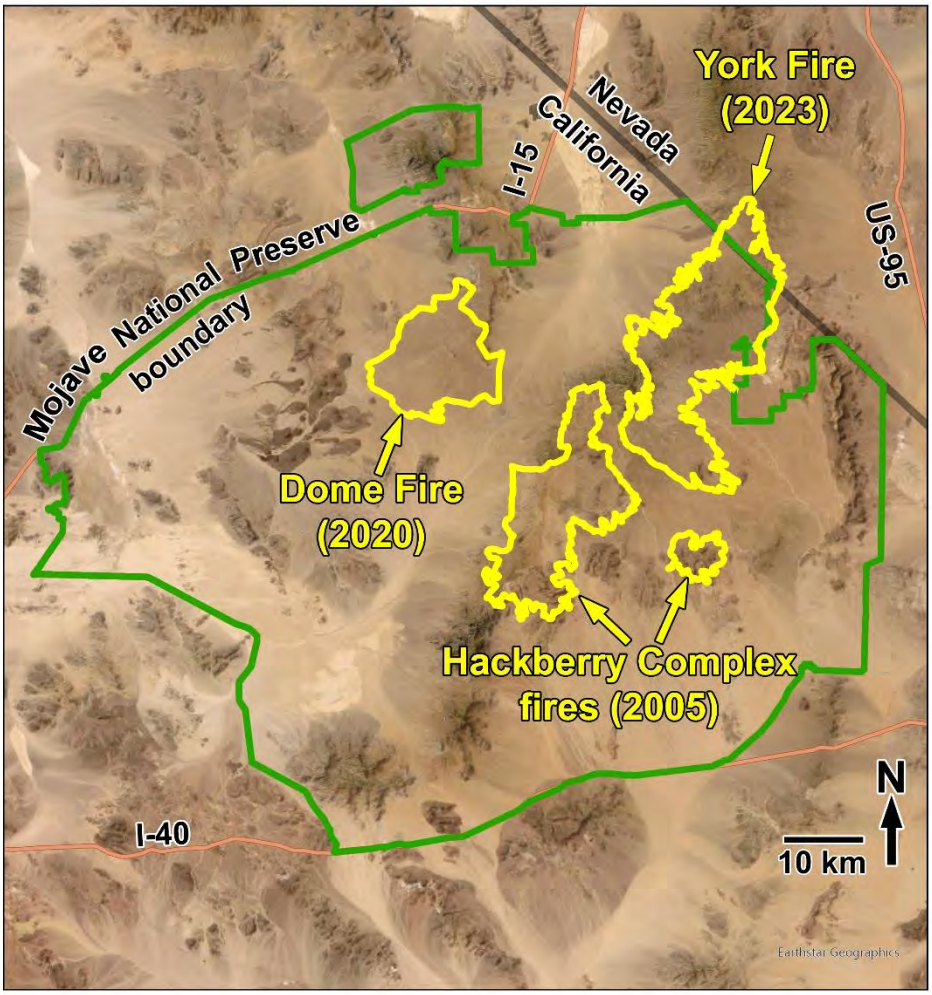


**Figure 1. Footprints of the three largest wildfires occurring within the last two decades in Mojave National Preserve, California. The 2023 York Fire extended northward into southern Nevada.**

News reports on the York Fire focused on several dominant themes: 1) the rapid spread and unprecedented size of the fire, which made it difficult to control, 2) attribution of the fire's spread to non-native plant species, specifically invasive annual grasses such as red brome (*Bromus rubens*), 3) destruction of native vegetation, particularly extensive stands of the iconic Joshua tree and pinyon-juniper woodlands, and 4) the lengthy process of ecological recovery and the possibility of long-lasting, even permanent vegetation change (*1-4*). Linking the spread and extent of the fire to an abundance of non-native annual grasses has continued to the present as a dominant theme (*5*). Attributing the large, recent wildfires in the Preserve to human-related impacts has been widely incorporated into public consciousness and concerns, as indicated by a statement in a 2024 membership drive by the Mojave Desert Land Trust:

> *"Mojave National Preserve is an area of global significance. It has suffered from large-scale wildfires, a recent phenomenon brought on by human impacts to the landscape."*

However, research conducted within the last decade indicates that prior to historical settlement times, wildfires occurred repeatedly in some types of vegetation in the Preserve, particularly in vegetation occupied by Joshua trees and junipers

[1] Desert Botanical Garden

[2] University of California Riverside.

within the area that burned in the York Fire. Recent wildfires in the Preserve, particularly the York Fire, need to be understood in the context of the fire regime before the historically recent era of Euro-American settlement (mid-late 1800s). In this article, we explore the following themes:

I Research regarding the timing and occurrence of wildfires within the footprint of the York Fire prior to the mid-1800s.
II Natural vegetation of the area and widely held misconceptions about its composition and ecological behavior.
III Fuels that were primarily responsible for the York Fire's rapid spread.
IV Extreme meteorological conditions with record-breaking periods of heat that were associated with the large, recent wildfires in the Preserve.
V Expectations for vegetation responses to the York Fire, as well as ways that future climate changes may affect the wildfire regime and vegetation.

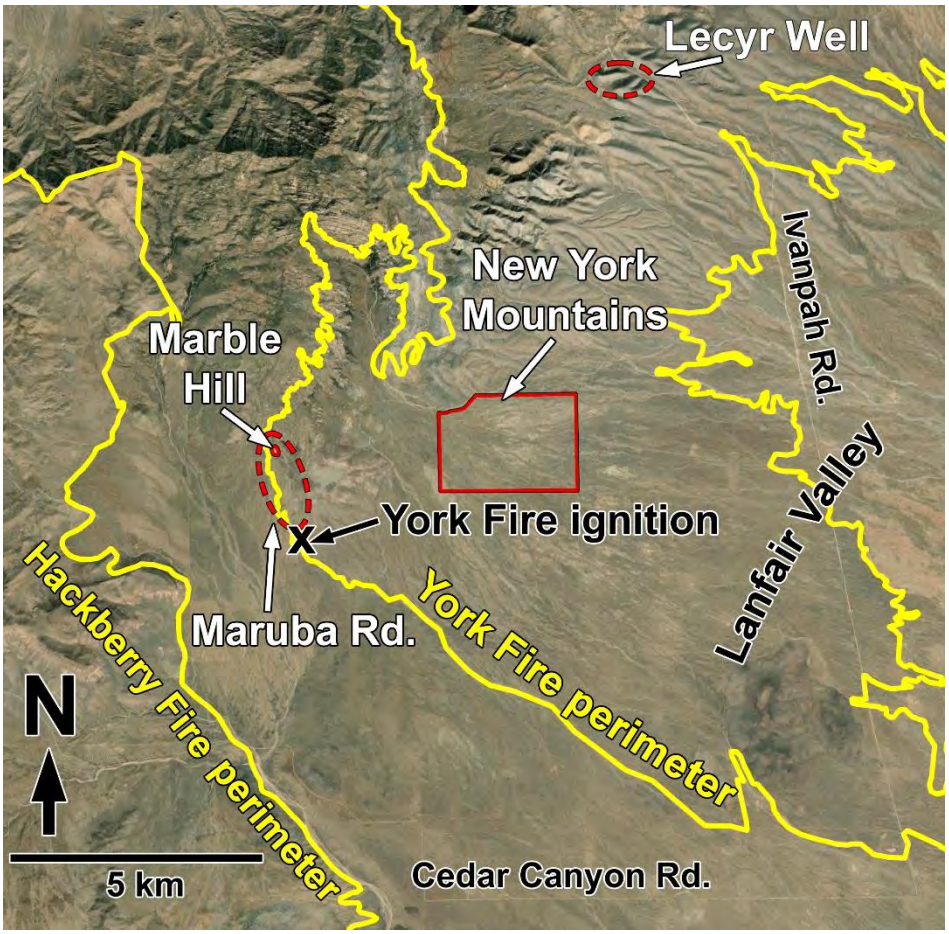


**Figure 2. Locations of study areas discussed in text. Areas bounded by solid red lines (New York Mountains, Marble Hill) are those where systematic surveys and mapping of all fire-hollowed remains of junipers were conducted. The two areas bounded in red dashed lines (Maruba Rd, Lecyr Well) are areas of general reconnaissance.**

**Theme I: Timing and occurrence of wildfires in pre-Euro-American settlement times in parts of Mojave National Preserve**

Evidence for the occurrence of wildfires long ago on the eastern side of the New York Mountains was initially reported by the first author in 2018 at the California Native Plant Society Conservation Conference (*6*), then, as an article in the 2020 Science Newsletter (*7*), and again in a presentation at Mojave National Preserve headquarters in March 2020 (*8*). In September 2021, the NPS subsequently funded the first author to conduct research on the history of wildfire in a portion of the Preserve (*9*). A final report for the fire history study will be available as a separate document; however, a brief summary of those results is pertinent, and therefore included, in this article.

The principal study site for the fire history investigation is a 2 x 2.5 km area on the eastern side of the New York Mountains, centered approximately 6.5 km west of the intersection of Ivanpah Road and New York Mountain Road (Fig. 2), and is within the area that eventually burned in the York Fire. From April 2017 through May 2019, this area was systematically surveyed for remains of junipers (*Juniperus osteosperma* and *J. californica*) consisting of fire-hollowed stumps and standing snags that may represent trees killed by past fires. The fire-hollowed remains of 664 dead juniper trees were located and mapped (*7*).

Sawn cross-sections of fire-hollowed stumps and dead snags were collected in 2018, 2021 and 2022 for the purpose of determining when those trees died. The fire-hollowed remains exhibit a wide range of decay and deterioration. The wood of many stumps is relatively intact and solid, retaining a considerable amount of the more decay-prone sapwood, traces of bark protected between woody lobes of the trunk, and fire-hollowed areas that retain solid, blackened, charred surfaces. Others exhibit considerably advanced decay, with sapwood nearly or entirely lost to insect damage and decay, extensive splitting and fragmentation of the wood, and fire-hollowed surfaces from which blackened char has been entirely removed by weathering (Fig. 3). These differences suggest the repeated occurrence of wildfires in the area over a long period of time.

An initial attempt to use dendrochronological dating methods to determine when those trees died was unsuccessful due to the lack of a suitable tree-ring master chronology for the area coupled with an inability to cross-date highly irregular tree-ring growth patterns of junipers from the site. Consequently, radiocarbon dating was employed, using a specialized approach called wiggle-match radiocarbon dating, in which separate radiocarbon ages are obtained from several

widely spaced growth rings from a tree. This approach is necessary because the radiocarbon age determination of a single sample (e.g., the outermost growth ring) often translates into periods of time that may span a century or more. This imprecision is due to the existence of reversals, plateaus and "wiggles" in the radiocarbon calibration curve, which represents the relationship between radiocarbon age and calendric age (e.g., calendar year) (Fig. 4). The calibration curve is an extensive compilation of radiocarbon ages of materials whose actual age in calendric years is precisely known. In particular, the radiocarbon calibration curve for the northern hemisphere for the last 10,000 years is based largely on radiocarbon dates of annual growth rings of bristlecone pine (*Pinus longaeva*) and other long-lived trees that exhibit regular annual ring production, and hence, the actual calendric year of ring formation is known (*10*).

The irregularities in the radiocarbon calibration curve are generated by variation in production of the radioisotope $^{14}C$ in the upper atmosphere from nitrogen-14 ($^{14}N$) due to cosmic ray bombardment. Multiple factors influence the level of cosmic ray bombardment, including solar variation, changes in the strength of the Earth's magnetic field, and even rarer cosmic events, like supernovae (*11, 12*). Additionally, from around 1700 A.D. to the present, the calibration curve exhibits a long, irregular plateau with two pronounced reversals of the relationship between radiocarbon age and calendric time (Fig. 4). One historically recent contributor to these irregularities has been the burning of fossil fuel from the time of the Industrial Revolution (mid-18th century) onwards, which releases carbon dioxide devoid of $^{14}C$ to the atmosphere (virtually all of the original $^{14}C$ fixed within organic matter millions of years ago has long since been lost to radioactive decay) (*11*). The periods of reversals, wiggles, and plateaus in the calibration curve, especially over the last 550 years (since the mid-late 1400s), make it impossible to derive a precise calendric age from a single sample of organic material produced within that time frame (Fig. 4). This is particularly relevant to the investigation of wildfire history in the Preserve, since remains of many of the fire-hollowed stumps and snags likely represent trees that died during the last several centuries.

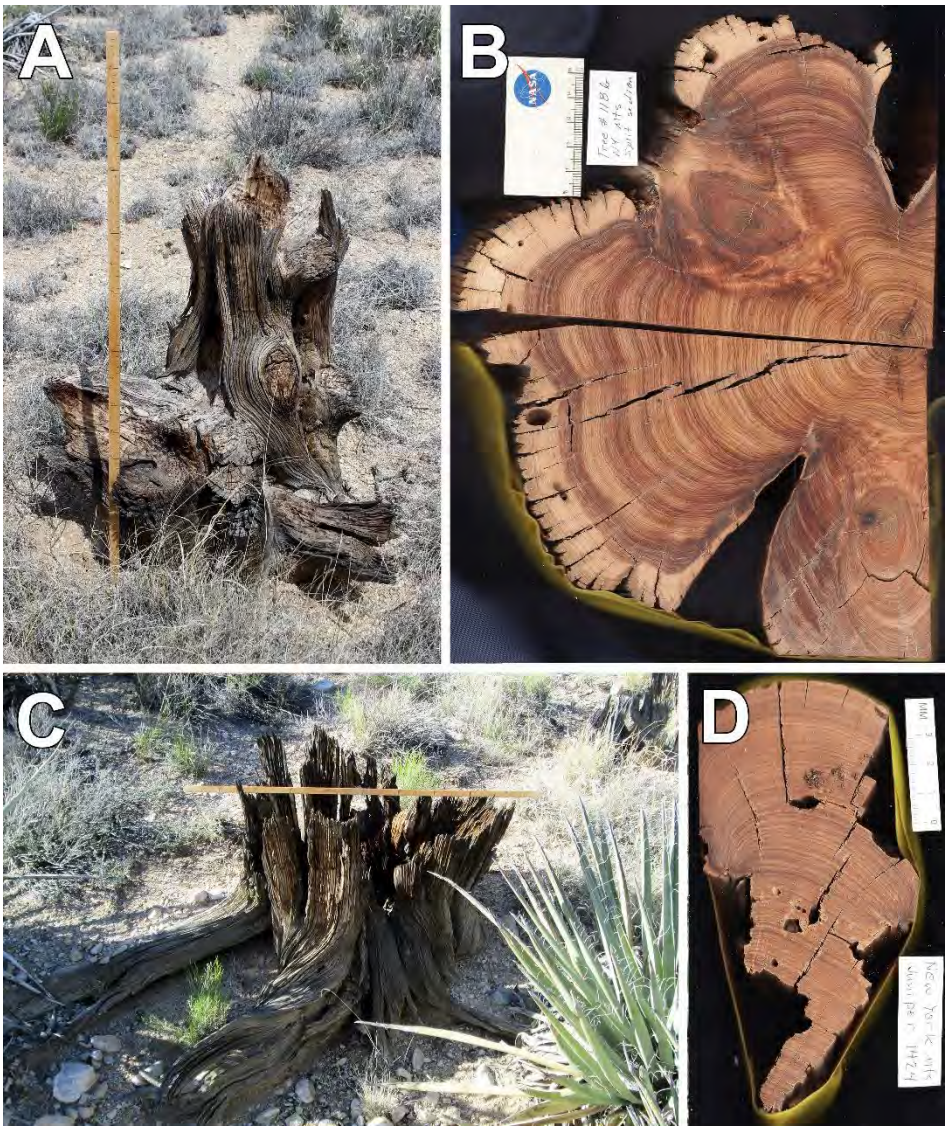


**Figure 3. Contrasts between the remains of two fire-hollowed juniper stumps from the New York Mountains study area. A. Juniper #118, consisting of a stump (50 cm basal diameter, 70 cm height) with fire-hollowed surfaces of stems. Blackened char was present on some surfaces of those hollows. B. Polished cross-section of Juniper #118 showing the largely intact perimeter of light-colored sapwood. C. Juniper #1424, consisting of an extremely weathered stump (70 cm basal diameter, 50 cm height) hollowed out by fire. The bottom surface of the bowl-like hollow in the stump contained small traces of charcoal, but the charred surface on the exposed parts of the hollow were completely lost to weathering. D. Polished cross-section of the best-preserved lobe of Juniper #1424 exhibiting substantial loss of wood to decay and insect damage. This section contained a 5 mm thick layer of darkly stained sapwood. All photos by J. R. McAuliffe.**

Wiggle-match radiocarbon dating provides an effective solution to the above problem (*12*). In practice, in order to determine the timing of tree death by dating the outermost wood in trees with annual growth rings, the growth rings of an entire cross-section are sequentially numbered from the innermost to outermost wood. Samples from several individual numbered growth rings, (e.g., inner, outer, and a centrally positioned ring) are removed for radiocarbon dating. Those measurements provide a set of radiocarbon ages whose separation from one another in calendric time (number of years) is known, based on their locations in the numbered

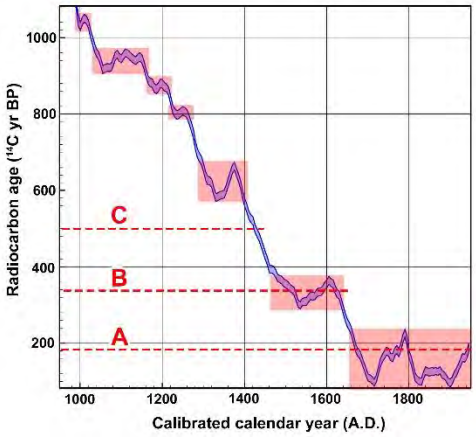


**Figure 4. Radiocarbon calibration curve from 1000 to 1950 A.D. The pink-shaded zones highlight periods of reversals, plateaus and "wiggles" in the curve that complicate the direct conversion of radiocarbon age measurements to calendar dates. For example, the pink-shaded period from approximately 1660 through 1950 A.D. exhibits a plateau-like shape within which irregularities occur, including two major reversals of the relationship between radiocarbon age and calendric time. As a consequence, plant material produced during any portion of this 300+ year period (e.g., an annual tree-ring) will carry a radiocarbon age signature that prevents a precise conversion to a calendar age. For example, the red dashed line labeled "A" represents a radiocarbon age determination (measured by the direct measure of the relative amount of $^{14}C$ versus stable carbon isotopes within the sample), but that measurement translates to calendar dates ranging from the late 1600s to the early 1900s because the red line crosses the calibration curve several times. A similar, but less extreme case occurs in the period from approximately 1460 to 1640. A radiocarbon age determination represented by the red dashed line labeled "B" translates into calendar ages that range over a century, from approximately 1500 through the early 1600s. A relatively precise conversion of a radiocarbon age determination to a calendar date is possible only in restricted areas of the calibration curve lacking plateaus and wiggles (e.g., the red dashed line labelled "C") because the red line only crosses the calibration curve in one place.**

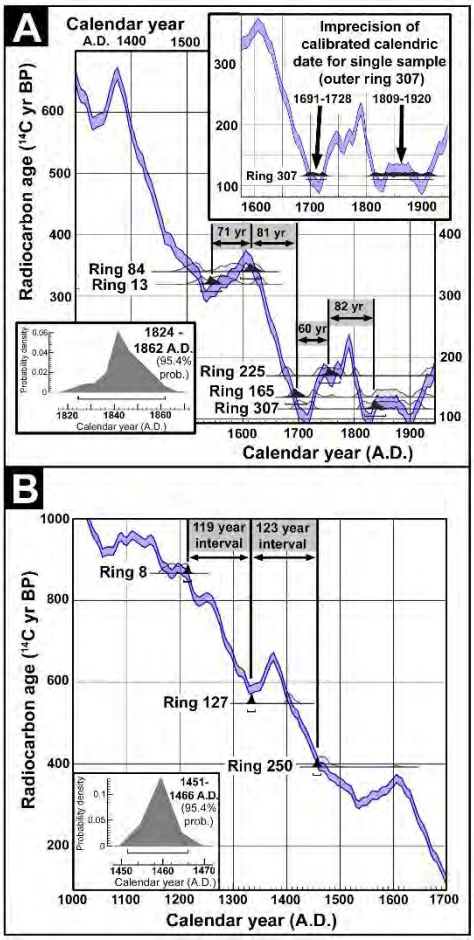


**Figure 5. (Left) A. Wiggle-match dating of Juniper #118 (pictured in Figure 3A, B). The small inset graph in the upper right shows a portion of the radiocarbon calibration curve demonstrating the lack of precision resulting from a radiocarbon determination of a single sample. In this case, the outermost ring sampled (Ring 307, counting from the pith outward) has a radiocarbon age that translates into a wide range of potential calendar ages, ranging from the late 1600s through early 1700s, and also from approximately 1800 to the early 1900s. However, a set of 5 separate growth rings (Ring 13 near the pith through Ring 307 near the outer surface) have a known separation in calendric time based on their sequential annual ring counts (separations of 71, 81, 60, and 82 years as indicated in the shaded boxes). Those intervals constrain the locations of radiocarbon age determinations along the calendric time (X) axis. Thus constrained, the set of radiocarbon age measurements assumes a shape that conforms to a unique segment of the overall radiocarbon calibration curve. In this case, the outermost Ring 307 has a calculated calendric age in the early 1840s ± 19 yrs (1824-1862). The inset graph in the lower left shows the probability distribution of the calibrated age of the outermost ring of the tree (= the calibrated age of Ring 307 plus 6 additional annual rings to outermost edge of sapwood).**

**B. Wiggle-match dating of Juniper #1424 (pictured in Figure 3C, D). Radiocarbon age determinations of three growth rings (Rings 8, 127, 250) were sufficient to enable wiggle-match dating of the outermost wood to within a highly precise, 15-year interval from 1451 to 1466 A.D. This precision would not be possible with a radiocarbon age determination from Ring 250 alone, which would have yielded a calendric age determination of approximately 1460, but also a statistical possibility of a date around 1600 due to the measurement uncertainty associated with the radiocarbon age of that ring (95% probability of 393 ± 22 radiocarbon years). The lower end of that probability range (393 – 22 = 371 radiocarbon years) intersects the sharp peak of the calibration curve just after 1600.**

sequence of annual growth rings. The radiocarbon ages of those rings plotted against their actual separation in calendar years takes the form of a small segment of the overall radiocarbon calibration curve. If the shape and elevation of that segment can be uniquely matched to a restricted portion of the overall radiocarbon calibration curve, a calendric age of the outermost growth ring can be established with relatively high precision, often within ± 20 years. Juniper trees may include missing rings, false rings, and incomplete rings that potentially complicate assignment of an accurate annual sequence of the rings. However, the wiggle-match dating approach can accommodate these irregularities to a degree, and reveal a pattern in the separation in time of radiocarbon dates that effectively constrains the period of calendric time during which the outermost wood was produced. This approach using radiocarbon dating cannot provide the temporal resolution that is possible with dendrochronological methods, in which timing of past wildfires can be precisely dated to specific years. Nevertheless, it provides a way to assess for the first time the general timing of wildfires that occurred in the past within the Preserve.

Funding for this project (*9*) allowed for radiocarbon dating of approximately 100 individual growth ring samples; however, a minimum of three to five growth rings per tree are typically required for the successful application of wiggle-match dating. Consequently, the project aimed to determine the timing of death of at least 20 trees. Cost of radiocarbon dating (~ $400 per individual radiocarbon date determination) represents a significant limitation to the number of trees that can be dated with this method (i.e., $1200 to $2000 per tree). The process of removing individual growth rings for dating was quite meticulous during this project because most growth rings were typically ≤ 0.5 mm in thickness. That work was done with the aid of a microscope, minute scalpels, and forceps, yielding samples of individual growth rings weighing a minimum of 20 milligrams. Surgical gloves were worn during this work to prevent contamination with "modern" carbon that is contained in body oils and perspiration. The radiocarbon dating analyses were performed by the University of Arizona's Accelerator Mass Spectrometry Laboratory, now a part

of the Laboratory of Tree Ring Research.

One priority in the wiggle-match radiocarbon dating effort was to determine the time of death of a series of fire-hollowed trunks that exhibited the least amount of decay and the least weathered burned surfaces. Remains in this condition were abundant and distributed across the northern half of the study area, and potentially represent more recent episodes of wildfire-caused tree death at the site. Each of the stumps sampled for dating had old, extremely weathered axe cuts superimposed on fire-hollowed surfaces, indicating removal of remaining, unburned stems from trees that had been previously damaged or killed by fire. Historical artifacts associated with the woodcutting activities indicated the time of wood harvest was shortly before 1900, most likely to supply fuelwood in the early 1890s for steam-powered equipment (multiple stamp mills, pumps, and hoists) at the newly established, but short-lived gold mining operations in Vanderbilt, located 13 km north of the study area (*7*). Traces of long-abandoned wagon trails through the area of woodcutting connect to an old wagon route to Vanderbilt. Wood removed for fuel was apparently limited to either fire-killed or otherwise dead and dry wood, reflecting an immediate and pressing need for well-seasoned wood to fuel steam-powered equipment of the mining operations. Wiggle-match dating indicates that the sampled trees died at broadly overlapping calibrated dates in the early 1800s, decades before harvest of remaining unburned wood. Three of the stumps, located within an area 1.2 km wide, died between 1805 to the late 1820s. The other two located in another area, but separated from each other by 0.25 km died sometime within a few decades after the mid-1820s (Fig. 5A). Although it is unknown whether fire killed those trees in the early-mid 1800s before harvest of wood, the harvest of fuelwood in the latter 1800s *after* damage by fire indicates the occurrence of one or more wildfires in the area during the 19th century.

Wiggle-match dating of other fire-hollowed stumps in the same area that were extremely weathered, including the loss of original charred surfaces on fire-consumed hollows, show that some trees died 500 or more years ago. Two trees located 0.45 km apart both died in the mid-late 1300s. The outermost growth ring of another extremely weathered, fire-hollowed stump dates to the mid-1400s (Figs. 3C and 5B), and time of death of others date to the 1500s and 1600s. Combined with the varying degree of weathering of the burned, fire-hollowed surfaces of these remains, these results provide evidence of the repeated occurrence of wildfire somewhere within the study area from around 1300 A.D. until the early- to mid-1800s, and occurrence of multiple fires over time in some places.

***Evidence of past wildfires from other nearby areas –*** Two additional areas within or bordering the footprint of the York Fire have been surveyed for evidence of past wildfires in the form of fire-hollowed juniper stumps. The first area was examined in 2017 before the York Fire occurred and consisted of north- and south-facing hillslopes 2 km south of Barnwell (labeled “Lecyr Well” in Fig. 2). The second area, searched in December 2023, was on the western boundary of the York Fire (labeled “Maruba Road” in Fig. 2), where unburned areas next to the burned area were examined. Additionally, within a burned portion of the “Maruba Road” area, a small unburned hill (labeled “Marble Hill” in Fig. 2) was surveyed and systematically mapped. Fire-hollowed stumps of junipers were distributed throughout all of these areas. Like the New York Mountain study area, those remains, including the original fire-hollowed surfaces, exhibited a range of weathering and decay, indicating fires at multiple times in the past (Fig. 6).

Homesteaders who occupied Pinto Valley in the early 1900s (the area of the surveys along Maruba Rd. described above) recognized that wildfires had occurred in the area long ago, based on their observation of standing dead, fire-hollowed juniper snags. An oral history provided in 1978 by Seth Alexander, who was 12 years of age when he moved to Pinto Valley in 1917 with his homesteading parents, records concern about the danger of wildfires, particularly those ignited by lightning, and his awareness that wildfires had occurred in the area long ago. The Alexander family homestead was located approximately 2 km directly west of the ignition site of the York Fire. Seth Alexander commented that standing remains of dead junipers bearing evidence of previous wildfires were harvested for firewood, and due to the decay-resistance of the wood, surmised that the trees had been killed by fires that occurred long ago: “*… and ‘course they don’t rot very fast, and they stood there for a century maybe…*” (*13*).

The York Fire occurred in an area where wildfires repeatedly occurred before the mid-1800s. Since then, large wildfires have apparently been absent until the 2023 York Fire. With the establishment of large-scale ranching operations in the mid-1890s, followed by the homesteading era of the first decades of the 1900s, Lanfair Valley, Pinto Valley, and Caruthers Canyon were extensively occupied and used. No historical records from that period record the occurrence of large wildfires. Likewise, there is no evidence on the ground in this area of the occurrence of large fires during this period. However, as pointed out previously, at least some of those early residents recognized that fires had occurred long before their arrival, as evidenced by old, fire-hollowed remains that were cut for fuelwood in the early 1900s. The relatively wildfire-free 20th century of this area is an anomaly, given the emerging evidence for the repeated occurrence of wildfires in many centuries leading up to 1900.

Cattle ranching operations in the area that began in the mid-1890s continued for slightly more than a century until 2000 (*14*). Evidence collected in ground surveys during the 1970s, as well as repeat photography before and after removal of livestock around 2000, reveal heavy and chronic over-use of the perennial grass vegetation throughout the area by livestock.

Those observations indicate that perennial grasses including *Hilaria rigida*, *H. jamesii*, and *Bouteloua eriopoda* were routinely consumed to within 1-2 cm of the ground surface in Lanfair Valley, as well as Cima Dome (*15, 16*). That persistent, heavy use essentially eliminated the types of fine fuels that would have played a central role in the repeated occurrence and spread of wildfires before the historical settlement period. The resurgence of native perennial grasses following the cessation of livestock grazing in Lanfair Valley and surrounding areas represents a restoration of the ecological condition that more likely resembles the original vegetation before the modern era of use and settlement. A sense of the nature of Lanfair Valley's perennial grass-dominated vegetation four decades before the ranching era commenced is revealed in daily notes by Lieutenant A.W. Whipple in 1854, in which he described the valley as a "prairie" and wrote "*The great plain which our route traversed was found to be covered with good grass," and "This country affords excellent grazing lands, similar to, but less extensive than those of New Mexico. The grass is highly nutritious.*" (*17*).

One aspect of wildfire dynamics that was present long ago in the area but is now absent is the purposeful "tending" of landscapes with fire by pre-Euro-American settlement inhabitants (the *Nuwuvi* or Southern Paiute peoples) (*18, 19*). This cultural group practiced intentional burning of landscapes to achieve multiple purposes, including enhancing productivity, reducing fuel loads with pinyon pine stands, and for hunting drives. Such practices probably occurred within the area of the New York Mountains and adjacent Lanfair Valley. Consequently, the pre-Euro-American settlement fire regime in this area was likely driven by climate-driven fuel loading, combined with ignition by either lightning or the intentional ignition of accumulated fuels by occupants of the landscape long ago (*20*).

**Theme II: Vegetation composition and expected ecological behavior**

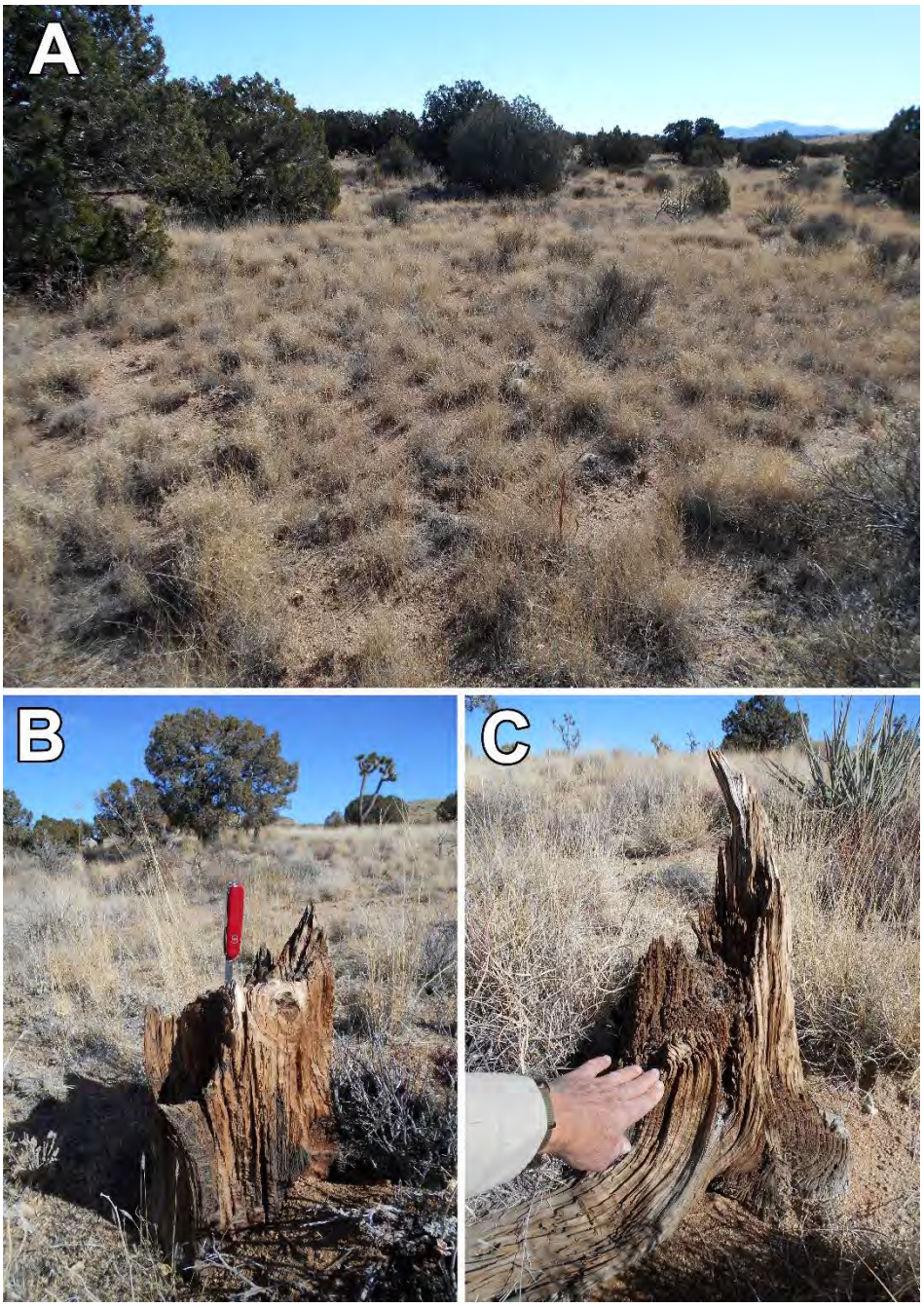


**Figure 6. A. Intact vegetation on the eastern side of Pinto Valley, just outside the western boundary of the York Fire and 1.7 km north of the ignition site. Relatively dense perennial grass occupies the area between widely spaced junipers; dominant grasses are *Hilaria jamesii* and *Bouteloua eriopoda*, with *B. gracilis* and *Muhlenbergia porteri* as minor components. Small amounts of red brome (visually estimated at well less than 1% total cover) were present at this site, with only four of 20 one-tenth meter square plots arranged along a transect containing that non-native species. B. and C. Two fire-hollowed juniper stumps apparently killed long ago in fires from the above location. The two stumps exhibit contrasting levels of decay; the stump in B exhibits relatively little decay and charred surfaces present within the fire-hollow. This contrasts with the more decayed and splitting remains in C, from which all traces of original char have been lost from the fire-hollowed trunk, indicating an earlier occurrence of fire compared to the fire that impacted the trunk in B. All photos by J. R. McAuliffe.**

Much of the Mojave Desert consists of shrub-dominated landscapes. However, substantial portions of Mojave National Preserve, particularly in the northern portion of Lanfair Valley on the east side of the New York Mountains that burned in the York Fire, are unique within the Mojave Desert due to the occurrence of vegetation in which native, warm-season perennial grasses contribute the majority of plant canopy and ground cover. In the upper elevations, widely spaced junipers

combined with the intervening cover of perennial grasses create a savanna-like appearance, while in the lower elevations, Joshua trees provide an arborescent component (Figs. 7A, B), and have been referred to as *Mojavean Juniper Savanna* and *Mojave Joshua Tree Savanna*, respectively (*15*). Dominant perennial grasses vary with elevation. Big galleta (*Hilaria rigida*), is most common in elevations below 1300 m (4265 ft.), but also occurs in mixed stands with black grama (*Bouteloua eriopoda*) at slightly higher elevations of ~1300-1500 m (4265-4920 ft.). *Bouteloua eriopoda* also occurs with galleta (*H. jamesii*) at higher elevations from 1400-1650 m (4590-5410 ft.), and at elevations above 1600 m (5250 ft.), blue grama (*B. gracilis*) commonly co-occurs with galleta (*15*). These perennial grasses have a $C_4$ photosynthetic pathway in which the optimum temperature for $CO_2$ uptake and photosynthesis is generally above 30°C (86°F) and decreases rapidly below 15° to 20°C (59-68°F) (*21, 22*). Consequently, these grasses require the regular input of warm-season precipitation in order to grow and reproduce.

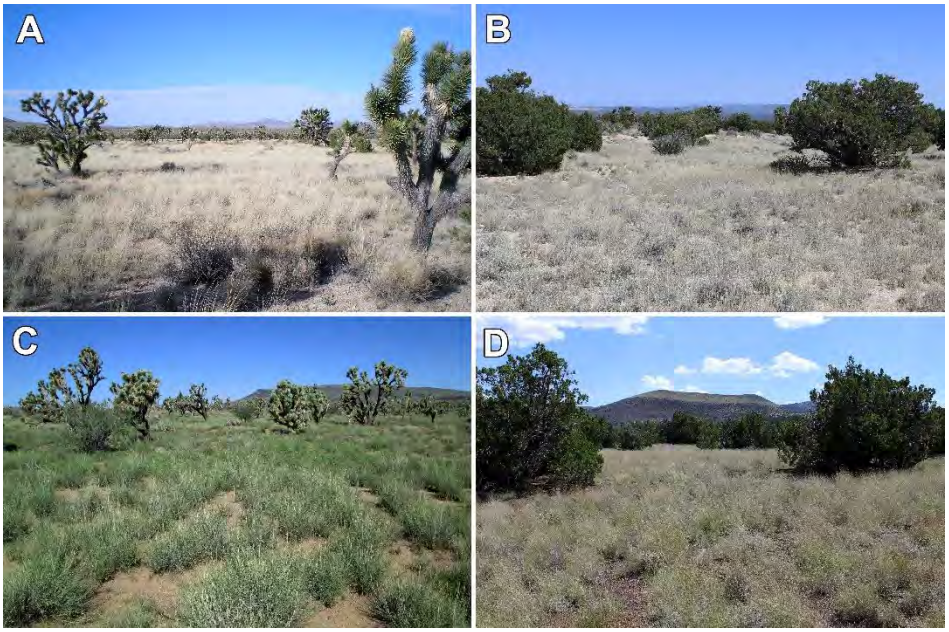


**Figure 7. These photos demonstrate the similarity of vegetation found in the East Mojave Highlands (A and B) and the warm-temperate "desert grasslands" of the American Southwest that extend further east into Arizona and New Mexico (C and D). Although the vegetation is nearly identical in the composition of dominant species and plant life-forms, they have acquired very different names depending on the vegetation classification being referenced. A. Predominant cover of perennial grasses (*Hilaria rigida* and *Bouteloua eriopoda*) and widely spaced Joshua trees in the 5 km² New York Mountains study area; 35.21680°N, 115.26262°W; elev. 1502 m, photo taken on 26 March 2013. According to recent vegetation classifications (*30, 35*) this would be assigned to the *Joshua Tree Wooded Shrubland Alliance*.**
**B. Widely spaced California junipers with native, warm-season perennial grasses forming bulk of cover between tree canopies. The predominant perennial grass species is *Bouteloua eriopoda*. Located within the New York Mountains study site; 35.21318°N, 115.27023°W, elev. 1531 m, photo taken on 10 April 2017. According to the recent vegetation classifications, this would be considered *Juniperus osteosperma/Shrub Understory Woodland Alliance*.**
**C. Mojavean Joshua tree savanna in Arizona consisting of Joshua trees in a matrix dominated by native perennial warm-season grasses, 9 km north-northeast of of Dolan Springs, Arizona, on the north side of the Cerbat Mountains, 100 km northeast of Lanfair Valley in the Mojave National Preserve. The dominant perennial grass is *Hilaria rigida*, with lesser amounts of *Bouteloua eriopoda* and *Muhlenbergia porteri*. The large shrub in front of the two Joshua trees on the left side is a catclaw acacia (*Acacia greggii*). The green color of the landscape is due to record-breaking precipitation from Tropical Storm Ivo approximately three weeks before the photograph was taken. 35.65957°N, 114.22173°W, elev. 1055 m elev., photo taken on 15 September 2013. According to a recent vegetation classification published for this area (*15*), this vegetation is designated as *Mojavean Joshua Tree Savanna*.**
**D. Juniper savanna in Arizona in the vicinity of Sunset Crater National Monument northeast of Flagstaff and 350 km east of Lanfair Valley in Mojave National Preserve. The dominant perennial grass is *Bouteloua eriopoda*, with lesser amounts of *B. gracilis* limited to areas partially shaded next to juniper canopies. 35.41744°N, 111.39948°W, elev. 1729 m, 17 August 2015. According to recent vegetation classification encompassing the entire distribution of pinyon-juniper woodlands in the American West (*26*), this vegetation is designated as *Juniper Savanna*. All photos by J. R. McAuliffe.**

A combination of geographic and topographic influences is responsible for the delivery of significant amounts of warm-season precipitation to this area. The Preserve is located near the transition to the Sonoran Desert to the southeast (Fig. 8), an area influenced by influx of summer moisture associated with the North American Monsoon. The proximity of the Preserve to this moisture source, combined with topographic relief, generates climatic and environmental conditions within most of the Preserve that differ considerably from the rest of the Mojave Desert to the north and west. Overall, the area within the Preserve is a pronounced topographic bulge that rises above the valley of the lower Colorado River to the east and drops off to the west to the trough containing Soda Lake, Silver Lake, and extending north-northwest to Silurian Valley and Death Valley. We refer to the area of higher elevation consisting of the New York Mountains, Mid-Hills, Providence Mountains, Cima Dome, Mescal Range, and the Clark Mountain Range as the *East Mojave Highlands* (*15*). The elevated topography of this area intercepts the flow of summer monsoonal moisture from the south and east. Consequently, annual precipitation in the *East Mojave Highlands* is distinctly bimodal, receiving moisture from both frontal storms during the winter and spring, and convective storms in the summer. Average annual precipitation amounts at Mitchell Caverns on the east side of the Providence Mountains (1325 m = 4350 ft. elevation) and Mountain Pass on the south side of the Clark Mountain Range (1430 m = 4700 ft. elevation) are 265 mm and 212 mm, respectively. At those two locations, approximately 40% of annual total precipitation is received during the six-month period (April-September) during which the perennial $C_4$ grasses are capable of active growth and includes the summer monsoonal period (*7, 15*). Lightning accompanying summer convective storms in the *East Mojave Highlands* is the principal cause of ignition of wildfires in this

region (*23*). In addition to the influx of monsoonal moisture, precipitation derived from occasional eastern Pacific tropical cyclones (*15, 24, 25*), which occasionally make incursions into the region, can contribute significant amounts of precipitation in the latter portion of the warm season. Recent examples include Tropical Storm Ivo, which delivered record amounts of precipitation to the region on a single day in late August, 2013, and Tropical Storm Hilary in August, 2023, which delivered 5-12 cm of precipitation throughout the Preserve. Warm-season precipitation declines abruptly to the west, northwest, and north in other portions of the Mojave Desert. With that decline, occurrence of the previously mentioned perennial $C_4$ grasses diminishes, and the *Mojavean Juniper Savanna* and *Mojavean Joshua Tree Savanna* vegetation disappears from the landscape.

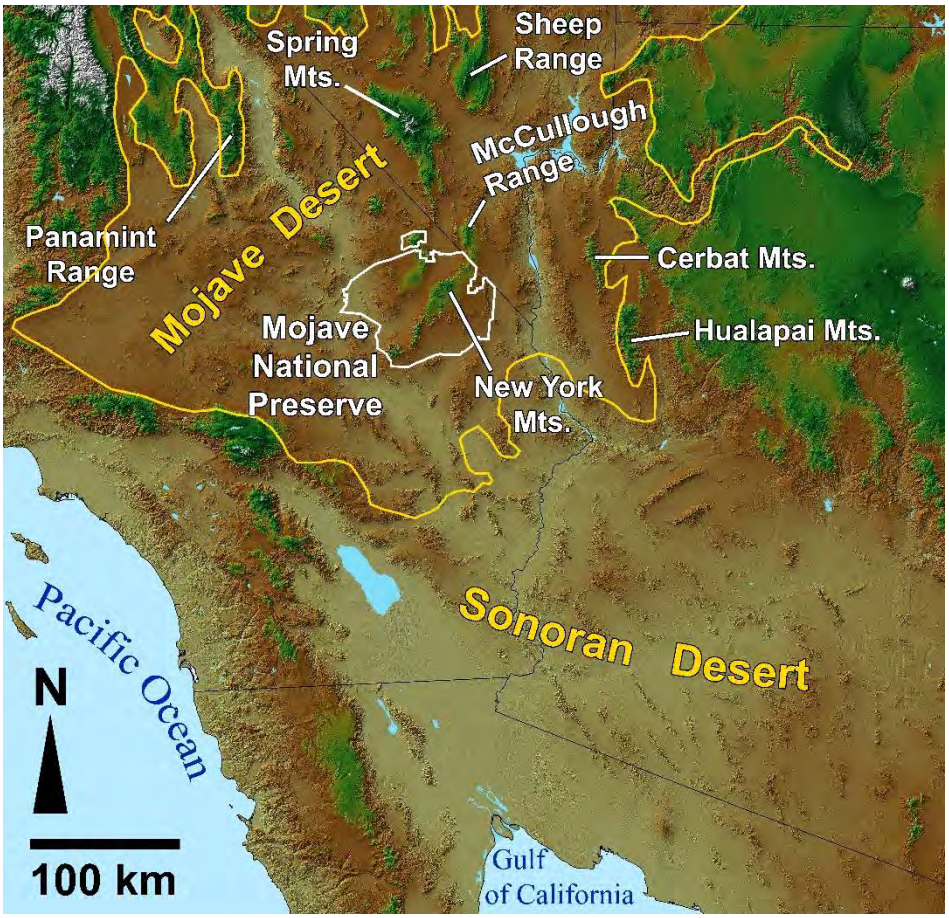


**Figure 8. Shaded relief map of the Mojave and Sonoran Desert regions. The boundary of Mojave National Preserve (MNP) is outlined in white. The topographic "bulge" referred to as the *East Mojave Highlands* includes the New York Mountains, Providence Mountains, Cima Dome, and the Clark Mountain Range. This elevated region intercepts the flow of moisture-laden air associated with the North American Monsoon, generating significant amounts of summer precipitation. Cool-season precipitation predominates in other parts of the Mojave Desert to the north and west. Baseline relief map created by Matthew P. King.**

Although this extensive area containing vegetation dominated by warm-season, $C_4$ grasses is unique within California, such vegetation is not restricted to the state but rather represents the western-most extension of warm-temperate grassland vegetation that is widely distributed throughout the American Southwest. For example, black grama (*B. eriopoda*) is one of the more characteristic perennial grasses of semi-arid grasslands throughout mid-elevations of Arizona and New Mexico and reaches the western limit of its distribution on the west flank of Cima Dome and the Clark Mountain Range. Vegetation that is nearly identical in species composition to the *Mojavean Joshua Tree Savanna* and *Mojavean Juniper Savanna* that predominate in Lanfair Valley on the east side of the New York Mountains and north to Castle Peaks and the Hart Mine area also occurs over 100 km to the east in Arizona in the vicinity of the Cerbat Mountains and Hualapai Valley north of Kingman (Fig.7C). Juniper savannas are geographically widespread and extend much further east into Arizona and New Mexico (*15, 26*) (Fig. 7D). The perennial grass-dominated landscapes within Mojave National Preserve represent the western-most "outposts" of warm-temperate "desert grasslands" of the American Southwest (*15, 27-29*).

Misconceptions about the composition of vegetation dominated by native perennial grasses in large portions of the area that burned in the York Fire probably contributed to some of the alarm expressed about potential ecological impacts of the fire. Names that do not reflect the actual character of the natural vegetation can foster such misconceptions. In 2004, the Mojave Desert Ecosystems Program of the U.S. Geological Survey (USGS), classified and mapped vegetation of most of the upper portion of Lanfair Valley to the east side of the New York Mountains as the "Joshua tree (*Yucca brevifolia*) Wooded Shrubland Alliance" (*30*) (Fig. 9). That designation was given to any vegetation in which Joshua trees accounted for ≥ 1% canopy cover, and "dominant understory species are shrub species such as *Coleogyne ramosissima*, *Opuntia ramosissima*, or the perennial grass *Pleuraphis* [= *Hilaria*] *rigida*." However, as noted above, those criteria fail to recognize the dominant perennial grass component (other than *H. rigida* in some cases), by overemphasizing the visually conspicuous Joshua trees. Further, by classifying the area as "shrubland" it fails to parse out the difference between vegetation with a dominant woody perennial component (i.e., blackbrush, *Coleogyne ramosissima*) from non-woody, perennial grass-dominated vegetation. The name shrubland is a significant misnomer of vegetation in Lanfair Valley and surrounding areas where widely spaced Joshua trees occur within dense

and extensive stands of native perennial grasses such as *Hilaria rigida*, *H. jamesii* and *Bouteloua eriopoda* (Fig. 9).

The names we apply to vegetation matter because they tend to reflect our views about ecological processes normally expected to occur in particular vegetation types. The Joshua tree is viewed as an iconic species and representative of the Mojave Desert region. That, coupled with evidence that historically, mid-elevation desert shrublands [e.g., those occupied by creosotebush (*Larrea tridentata*), blackbrush (*Coleogyne ramosissima*), or other shrubs that are not adapted to fire] were not prone to frequent or large wildfires before the spread of non-native, annual grasses (e.g., *23, 31*), the name "*Joshua tree wooded shrubland*" conveys an implicit message that fire is therefore undesirable within these vegetation types. In contrast, the designations of "grassland" or "savanna" carry with them the general perspective of wildfire as a natural and essential process that serves to maintain these ecosystems (e.g, *32-34*). Although the name *Joshua tree grassland* was applied to the vegetation of this area by an ecologist in the 1970s (*27*), that more fitting terminology was not incorporated into the more recent vegetation classification and mapping effort by the USGS.

In 2020, and again in 2024, the USGS vegetation classification for the Preserve was updated (*35-37*). Some classification criteria were slightly changed, but the name "Joshua Tree Wooded Shrubland Alliance" was retained for vegetation dominated by perennial grasses where canopy cover of Joshua trees was ≥ 2%. However, that designation continued to combine associations that contrasted greatly in the composition of understory vegetation, specifically associations with a woody understory component (e.g., blackbrush) and those with a non-woody perennial grass component (e.g., *Bouteloua* spp. and *Hilaria* spp.), classifying both as "wooded shrublands" (*36*). Although the 2024 update (*37*) included designation of a new "Joshua Tree/Big Galleta Wooded Grassland"

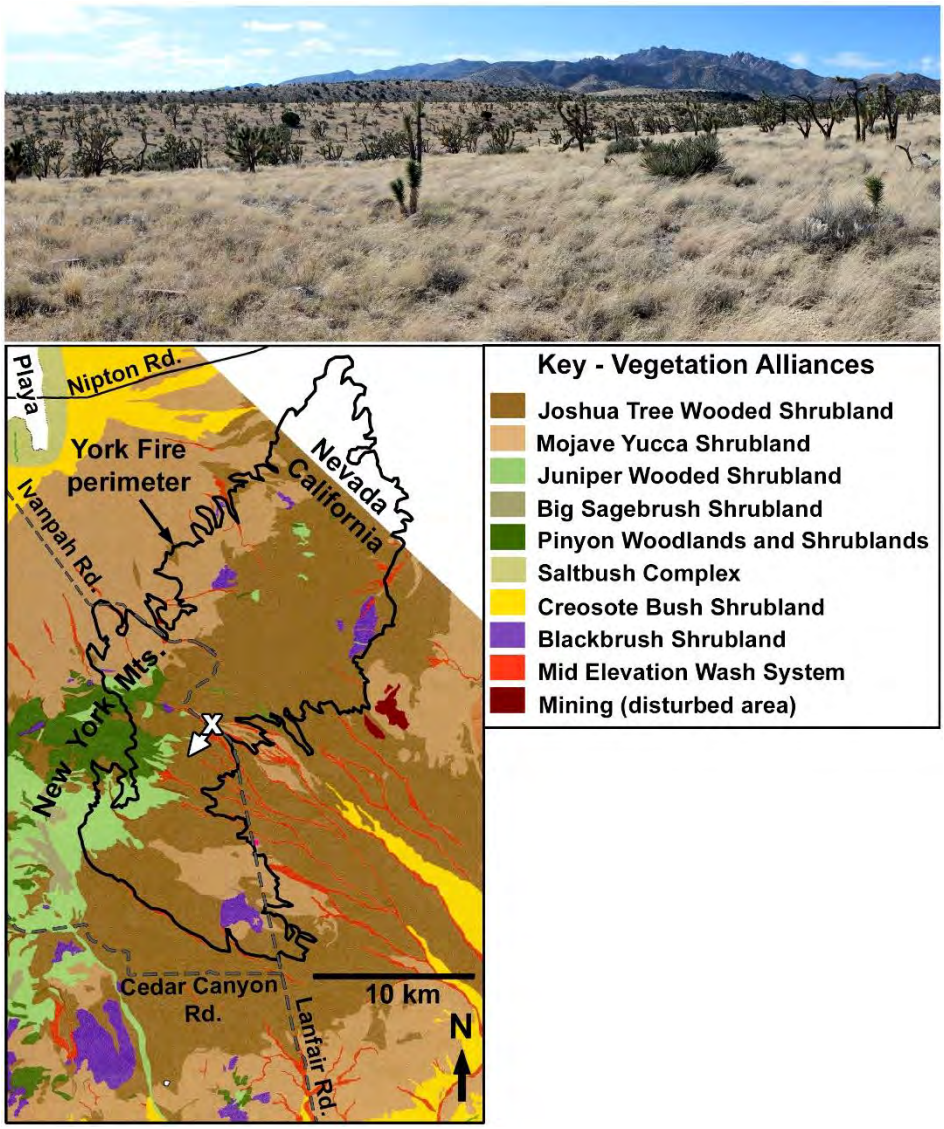


**Figure 9. Panoramic view of the alluvial piedmont flanking the east side of the New York Mountains (in background) shown in the upper panel (photo taken 25 October 2014 by J. R. McAuliffe) with a map of vegetation alliances found within the footprint of the York Fire shown in the bottom panel. The camera location and direction (35.26657°N, 115.23077°W) is indicated with the white "X" and arrow in the map. Vegetation of the entire foreground to mid-ground consists of widely scattered Joshua trees within a matrix of native perennial grasses, principally *Bouteloua eriopoda* and *Hilaria jamesii*. The entire landscape from foreground to mid-ground contains this kind of perennial grass-dominated vegetation. At higher elevations near the mountains, junipers rather than Joshua trees contribute the arborescent component to this savanna-like vegetation. This view shows the area through which the York Fire spread rapidly to the north on the second day of the fire. The vegetation alliance map shows the names and distributions of vegetation alliances designated in the 2004 USGS *Central Mojave Desert Vegetation Mapping Project* (*30*). According to the vegetation map, and also the 2020 update (*35, 36*), the area in the photo would be considered "Joshua Tree Wooded Shrubland Alliance," which does not accurately portray the perennial grass-dominated landscape.**

species association, that designation remained grouped within the overall "Joshua Tree Wooded Shrubland Alliance" together with seven other species associations in which woody shrubs (e.g., *Coleogyne ramosissima*, *Larrea tridentata*, *Artemisia tridentata*, and others) were dominant associates of the Joshua tree.

Similarly, vegetation at slightly higher elevation in Lanfair Valley and Pinto Valley next to the New York Mountains that consists of widely spaced junipers (*Juniperus californica* or *J. osteosperma*) within a relatively dense matrix of native warm-season perennial grasses was designated and mapped by the USGS as "Juniper (*Juniperus* spp.) Wooded Shrubland Woodland Alliance" (*30*). The 2020 and 2024 vegetation classification

update (*35-37*) similarly designated this vegetation as either "*Juniperus californica* Mojave Scrub Alliance" or "*Juniperus osteosperma*/Shrub Understory Woodland Alliance." Those names do not accurately reflect the actual composition of the savanna-like vegetation (as shown in Figures 6, 7, 12, 13, and 15). Referring to the large areas of perennial grass-dominated vegetation containing widely spaced junipers within the Preserve as "wooded shrublands" significantly mischaracterizes vegetation composition and by extension, dominant ecological processes that are expected to occur within them (*15, 26*). It is unfortunate that the more geographically comprehensive perspectives of other researchers were not incorporated into the more recent updates of vegetation classification for the Preserve. In particular, ecologists recognize three different types of pinyon-juniper woodlands (including stands of either pinyon or juniper alone) in the American West: (1) *persistent woodland*, characterized by dominance of trees and a sparse understory plant cover; (2) *wooded shrublands*, dominated by shrubs with varying densities of trees; and (3) *pinyon-juniper savannas*, where perennial grass cover predominates in spaces between widely spaced trees (*26*). Pinyon-juniper wooded shrublands have very different behaviors with respect to wildfire compared to pinyon-juniper savannas, with more frequent and regularly occurring fires in savannas (*26, 38*). Evidence in the form of hundreds of old fire-hollowed remains of juniper trees distributed throughout several study areas within what is now the footprint of the York Fire indicates that the area repeatedly experienced wildfire before the mid-1800s. The native, perennial grass vegetation of these areas was most likely the principal fuel responsible for wildfire spread, long before the introduction and spread of non-native, annual grass species.

**Theme III: What fueled the York Fire's rapid spread?**

As mentioned previously, the rapid spread and size of the York Fire has been widely attributed to the presence of non-native,

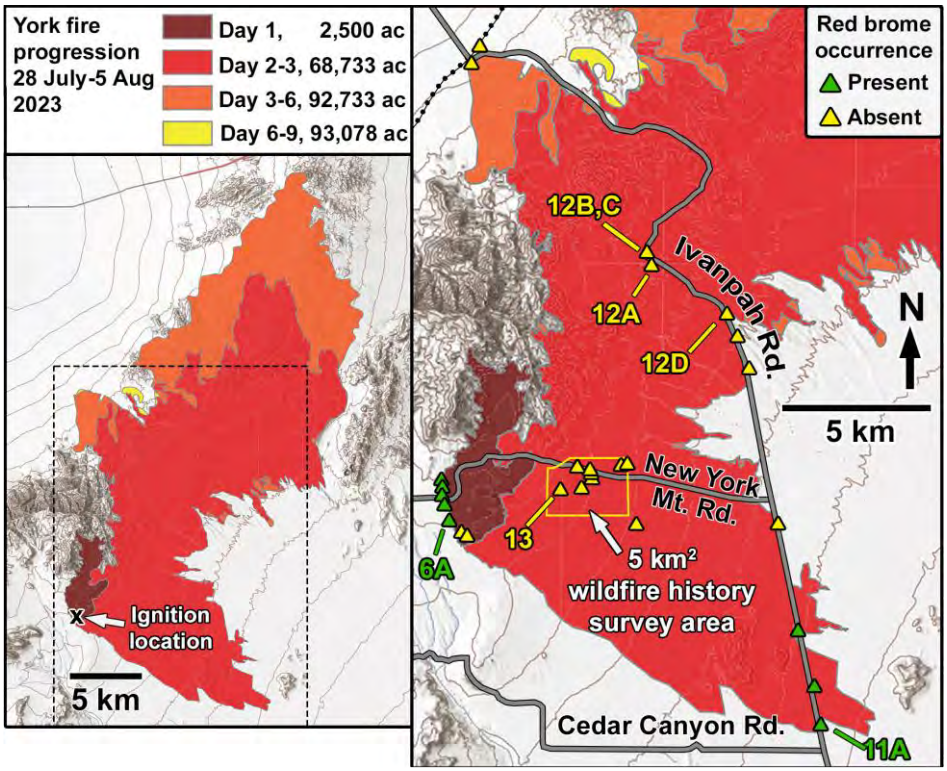


**Figure 10. Fire progression map of the York Fire (left panel) with an enlarged view of the dashed rectangle shown in the right panel. Ground survey sites (triangles) of unburned vegetation next to and within the footprint of the York Fire were conducted in November and December 2023. Sites with red brome present (≥ 1 individual plant) are shown in green, whereas yellow indicates sites where red brome was entirely absent. Corresponding ground photos are found for 6A, 11A, 12A, 12B, 12C, 12D, and 13 in figure numbers 6, 11, 12, and 13. (Fire progression map provided by James Aragon, BLM).**

invasive plant species such as red brome. For example, in the 4 April 2024 online meeting on fire management in the Preserve, organized and hosted by the NPS, the statement "invasive fuels carried a 7-mile flame front" was used when describing the fire's rapid spread in a northerly direction during the second day (*39*) (Fig. 10).

In parts of both the Mojave and Sonoran Deserts, non-native plant species have significantly added to fine fuel loads and an increased occurrence and size of wildfires in some places (*23, 40-42*). In the shrub-dominated portions of these regions, the growth of cool season, non-native grass species, particularly red brome, along with a few other non-native species, combined with many native ephemeral species, can produce an abundance of fine fuel that fills spaces between widely spaced shrub canopies, increasing the risk of rapid fire spread. Although this phenomenon occurs, a relationship between non-native species and wildfire spread has often been uncritically accepted as the general cause of all wildfires throughout the region. The widespread occurrence of hundreds of old fire-hollowed juniper trunks within the New York Mountains study site and other nearby areas provides evidence that wildfires repeatedly occurred in the area long before the arrival and spread of non-native species. The relatively dense growth of native perennial grasses of the area naturally fosters the occurrence and spread of wildfires with or without the presence of non-native species.

Lacking information about pre-fire conditions, particularly on plant density and species composition, it can be difficult to critically assess the nature of the fuels once a fire has consumed the vegetation. However, in some cases the types of fuels that were available can be assessed by examining adjacent areas and islands of vegetation that escaped burning due to the occurrence of firebreaks provided by natural and manmade features. This approach was

used previously by the first author to demonstrate the widespread occurrence of red brome produced in the cool season preceding the 2020 Dome Fire, providing evidence for the potential contribution of red brome in the spread of that fire (*43*).

In November and December 2023, areas of unburned vegetation within and immediately surrounding the footprint of the York Fire were examined to determine the nature of fine fuels that were available in those places at the time of the fire. Included were (1) areas along Ivanpah Road, from near the intersection of Cedar Canyon Road to the Ivanpah railroad crossing, near the fire's west-central limit, (2) unburned islands of vegetation within the 2 x 2.5 km wildfire history study area along New York Mountain Road, and (3) along Maruba Road, directly north of where the York Fire was ignited (Fig. 10). Areas in the northern half of the footprint of the York Fire were not examined, due to closure of access to this area after the fire.

Red brome produced during the winter-spring season of 2022-23, before the York Fire, could be readily identified, as could the native annual, warm-season grasses, primarily consisting of six-weeks grama (*Bouteloua barbata*), produced in summer of 2022 and summer of 2023 after the York Fire occurred (Fig.11). Based on the surveys conducted in December, 2023, the places where red brome occurred were limited to five of eight locations north of the ignition location along Maruba Road, and the southernmost extent of the fire near the intersection of Cedar Canyon and Ivanpah Roads (Fig. 10). At the locations along Maruba Road, the amount of fine fuel provided by red brome was extremely small (visually estimated at < 1% of all canopy cover) compared to that provided by standing crops of native perennial grasses (Fig. 6A). In the two southernmost locations along Ivanpah Rd., the growth of red brome was considerably greater, particularly below and within areas occupied by perennial plants, including big galleta and small shrubs such as Cooper's goldenbush (*Ericameria cooperi*), where it contributed up to a quarter of all fine fuels in some places, estimated visually (Fig. 11). Such growth would have contributed to fine fuel loading and fire spread in that particular area. However, further north from near the intersection of Ivanpah and New York Mountain Roads, and throughout the area where the fire rapidly spread northward and crossed Ivanpah Road on the second day of the York Fire, red brome was entirely absent from all areas examined (Figs. 10 and 12). All islands of unburned vegetation within the 5 km$^2$ wildfire history study area described previously completely lacked red

**Figure 11. Top photo shows vegetation on the east side of Lanfair Road, 1 km north of intersection with Cedar Canyon Road (Location 11A in Figure 10). At this location, Lanfair Road served as a firebreak preventing the eastward spread of the York Fire. Red brome produced in the cool season of 2022-23 was moderately abundant at this site and was largely confined to areas in and around canopies of perennial plants, including *Hilaria rigida*, *Ericameria cooperi*, and *Ephedra nevadensis*. 35.13610°N, 115.18613°W, 1247 m elev. 18 November 2023. Ephemeral grasses at the site at the time of the photograph included, from left to right in lower photo: *Bouteloua barbata* produced during the summer of 2022; *Bromus rubens* produced during the winter-spring of 2022-23; and *Bouteloua barbata* produced in summer, 2023, after the York Fire occurred (so would not have contributed to the fine fuel feeding the fire). Photos taken on 18 November 2023, 35.13610°N. 115.18613°W, elev. 1247 m by J. R. McAuliffe.**

brome (Fig. 10). Instead, the principal fine fuels in these islands consisted of standing crops of native perennial grasses, including *Hilaria rigida*, *H. jamesii*, and *Bouteloua eriopoda* (Fig. 13). The escape of those areas from burning in the York Fire is attributed to breaks in the density of vegetation cover associated with natural features, such as ephemeral stream channels, combined with the rapid movement of the fire on the second day. The northernmost site examined, located along the western limit of the York Fire's footprint near the railroad crossing at Ivanpah, is a lower elevation site characterized by desert scrub vegetation (*Larrea tridentata*, *Ambrosia dumosa*, and other shrub species, together with *Yucca schidigera* and *Opuntia basilaris*). Red brome produced in the winter-spring of 2022-2023 was entirely absent (Fig. 10), and the only annual grass available as fine fuel in summer 2023 was a profuse crop of *Bouteloua barbata*, produced in the previous summer of 2022.

The complete absence of red brome from the locations examined within the 5 $km^2$ study area, and also to the north along Ivanpah Road indicates that relatively dense stands of native perennial grasses throughout that area, not red brome, were principally responsible for the rapid, northerly spread of the fire across this area on the second day. Although rapid and extensive spread of the fire has been repeatedly attributed to the abundance of non-native annual grasses, the surveys conducted following the fire do not support that conclusion.

The substantial, dry and dormant standing crop of native perennial grasses present throughout the area was more than sufficient to foster the spread of the York Fire under the extreme meteorological conditions that occurred. The summer of 2023, up to the day of ignition of the York Fire, was dominated by extreme heat and aridity, and monsoonal precipitation had not arrived. The summer rains of 2022 fostered substantial growth of the native perennial grasses in the area but by the end of July, 2023 when the York Fire was ignited, the persistent, standing perennial grass biomass was dry and flammable.

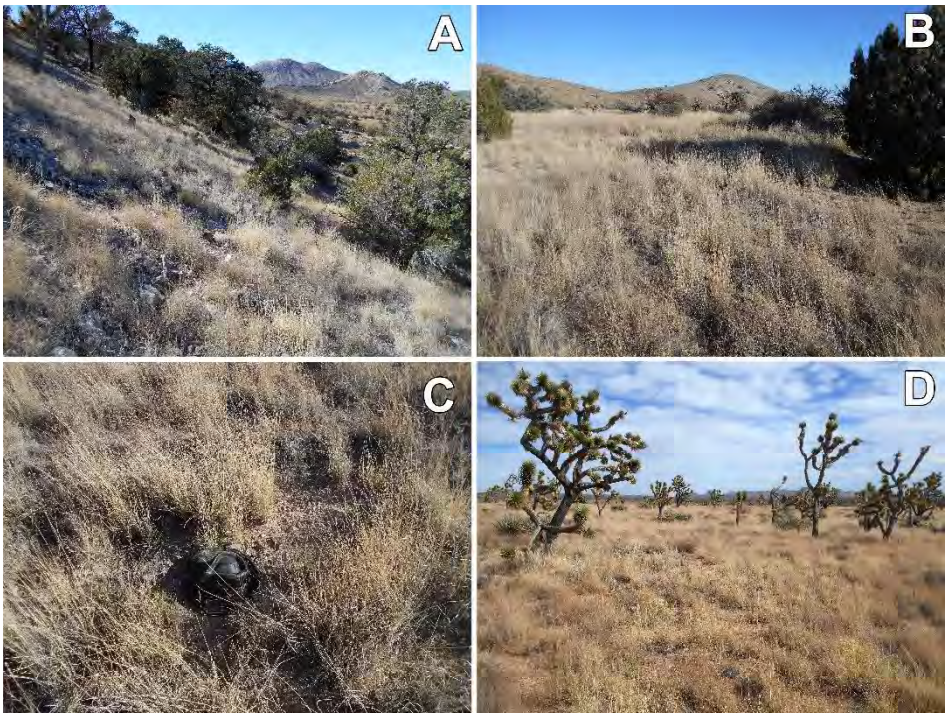


**Figure 12. Examples of unburned patches of vegetation that completely lacked red brome, but were dominated by native, perennial warm-season grasses. Locations are either within or next to the fire's footprint and were protected either topographic features or roads that served as fire breaks. Photo points are indicated as 12A-D on the map in Figure 10. All photos taken on 12 November 2023 by J. R. McAuliffe. A. North-facing hillslope east of Lecyr Well and 0.2 km southwest of Ivanpah Road. *Bouteloua eriopoda* and *Hilaria jamesii* predominate in the foreground; red brome (*Bromus rubens*) was absent from all unburned areas on this hillslope. View is northwest from 35.27538°N, 115.24707°W, elev. 1527 m. elevation; 12 November 2023. B. Unburned vegetation near the base of the hillslope pictured in A; closely spaced roads enclosed this area and served as a firebreak. Dominant grasses are *Hilaria rigida* and *Bouteloua eriopoda*. Red brome is absent, 35.27924°N, 115.24890°W, elev. 1500 m. C. Close-up, overhead view of vegetation in B with hat for scale, showing complete absence of red brome. D. Unburned vegetation on the northeast side of Ivanpah Road, which served as a firebreak, stopping its spread to the opposite side of the road. *Bouteloua eriopoda* and *H. jamesii* collectively provide approximately 65% total ground cover, with shrubs (*Krascheninnikovia lanata*, *Ephedra nevadensis*, *Psilostrophe cooperi*, and *Tiquilia canescens*) contributing only a few percent total canopy cover. Although Joshua trees are visually dominant, they contribute less than 2% total canopy cover; native perennial grasses are by far the dominant species at the site in terms of cover and total vegetation productivity. Red brome was entirely absent from the area. 35.26083°N, 115.21938°W; elev. 1433 m.**

**Theme IV: Extreme meteorological conditions and wildfire occurrence in Mojave National Preserve**

Over the past several decades, precipitation has varied considerably across the Preserve. Prior to 2020, the driest interval on record for the region was the water year of 1 July 2001- 30 June 2002, when the entire eastern Mojave Desert received only 10-20% of average annual rainfall. Some lower elevations did not record even a trace of precipitation during that 12-month period, and plant ecologists were surprised at the impacts on shrub and tree species. For example, vast areas at lower elevations just south of the Preserve saw nearly 100% mortality of brittlebush (*Encelia farinosa*), and California juniper (*Juniperus californica*) suffered 15-20% mortality near Granite Pass in the Preserve. The impacts of this drought extended beyond the Preserve, with 100% mortality of *Ambrosia dumosa* and nearly two-thirds of *Larrea tridentata* at one location in Joshua Tree National Park (*44*).

The 24-month period from July 1, 2020 through June 30, 2022 was another extraordinarily dry period for the region, as shown in the 38-year precipitation record from the University of California's Granite Mountains Desert Research Center

(GMDRC), located in the southwestern corner of Mojave National Preserve (Fig. 14). In fact, the back-to-back extreme dry years of 2020-2022 generated far more shrub mortality than the single extreme dry year of 2001-2002. While we are still assessing the impact of this severe drought, preliminary estimates from long-term plots at the GMDRC show 30-35% mortality in buckhorn cholla (*Cylindropuntia acanthocarpa*), Cooper's goldenbush (*Ericameria cooperi*), and Mojave cottonthorn (*Tetradymia stenolepis*), and 25-30% mortality in hollyleaf cherry (*Rhamnus ilicifolia*) and California juniper. One month prior to the York Fire, at a location in the eastern New York Mountains, approximately 40% of the California juniper were dead or dying as a result of the 2020-2022 drought (Fig. 15). The standing dead woody biomass of California juniper and other woody species no doubt provided additional fuel for the York Fire.

The recently coined term "hot drought" has been used to describe conditions where a given location experiences the concurrence of anomalously hot conditions and anomalously low precipitation (*45*). In recent studies, daily temperature extremes have been found to enhance fire ignition and rate of spread (*46*). While the drought of 2020-2022 primed the woody fuel to burn within the York Fire footprint, an unprecedented heatwave occurred during the weeks leading up to the ignition of the fire on 28 July 2023. Examining the 10 hottest months recorded at the GMDRC in the past 37 years (1987-2023), July 2023 clearly stands alone as extreme (Fig. 16). The average daily maximum temperature that month was 97.1° F, which is generally 3° F hotter than the other hottest months, and 5° F hotter than the long-term average high for July. Interestingly, the second hottest month shown in Figure 16 was August 2020, the month the lightning-ignited Dome Fire on Cima Dome occurred. For perspective, over the past 37 years only 62 days have reached or exceeded 100° F at the GMDRC. Of those, more than half occurred in July 2023 and August 2020 (17 and 15 days, respectively), coinciding with two of the three largest recorded fires in the Preserve (Fig. 16).


**Figure 13. Repeat photography of a location within the New York Mountains study area; New York Mountains in the background (location 13 in Figure 10). *Hilaria rigida* and *Bouteloua eriopoda* provide the dominant ground cover; red brome was not recorded on the 2018 date and detailed inspection on 14 November 2023 also demonstrated its absence. Approximately 50 m in front of the camera location, the fire passed from left to right. The area burned is in the mid-ground, just beyond the green, spherical juniper canopy at left center. The junipers and Joshua trees in this portion of the burned landscape were not completely consumed by fire, but rather can be identified by the browned, heat-killed foliage of their canopies. The rapidly moving fire apparently quickly exhausted the fine fuel supply provided by grasses, thereby reducing the intensity, heat, and destructiveness of the blaze. 35.20802°N, 115.28144W; elev. 1653 m.**

**Theme V: Expected future conditions in areas of the Preserve affected by wildfire**

The restoration of native perennial grasses

as a dominant component of the vegetation in some areas within the Preserve brings with it the potential return of a regime with recurrent wildfire as an integral, natural process that reinforces the predominance of those fire-adapted grasses. Previous smaller fires in the Preserve (e.g., the 1994 Lanfair Fire and the 65-acre Valley View Fire of 2006 on Cima Dome) substantially reduced shrub cover, particularly that of short-lived, unpalatable species such as *Ericameria cooperi*, leading to an increased predominance of native perennial grasses (*15, 43*). A similar trajectory can be expected for much of the area impacted by the York Fire. Concern has been expressed regarding the future of Joshua trees in the Preserve, and whether recurrent wildfires might eventually eliminate this iconic species from the landscape. Many Joshua trees do succumb entirely to wildfire, and observations following wildfires clearly show reductions in population densities in both the Preserve (*43*) and Joshua Tree National Park (*47*). It has also been suggested that the extremely high densities of Joshua trees in parts of the Preserve may actually be a byproduct of a century of overgrazing, as this reduces the perennial grass component, allows an increase of less palatable, shrubby vegetation cover, and enhanced opportunities for Joshua tree seedlings to survive (*14*). Within the 5 km$^2$ wildfire history study area on the east side of the New York Mountains (Fig. 2), observations throughout the entire area from 2017 through 2021 indicated the rarity of tall, old Joshua trees exceeding 6 m, and the abundance of considerably smaller, younger plants (JRM personal observations). This can be explained as a direct consequence of absence of wildfire from that environment for over 150 years, during which greater numbers of young individuals established and survived than would have under the previous regime of recurring wildfires. Without question, the density of Joshua trees throughout the footprint of the York Fire will be diminished for many decades to come from what was formerly present. However, that lower density may actually more closely resemble what would have been present when occasional wildfires occurred in the centuries preceding the mid-1800s.

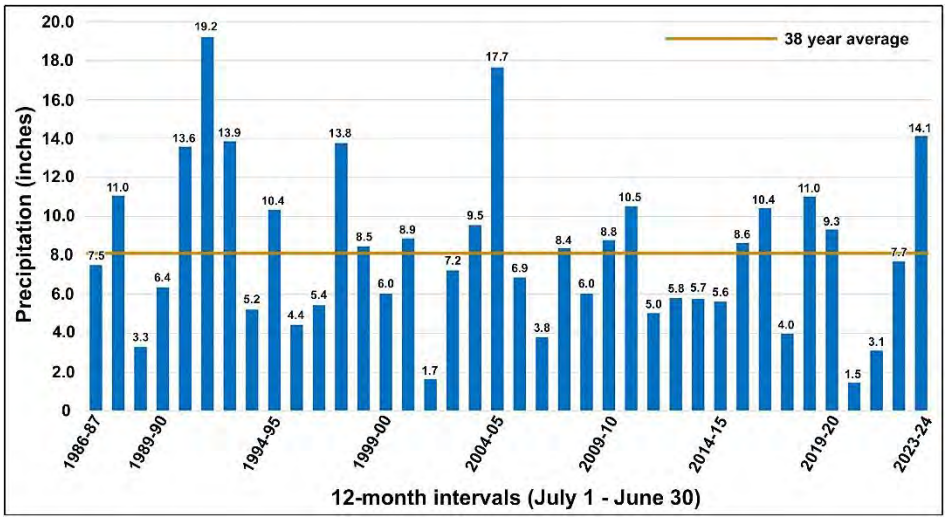


**Figure 14. 38-year precipitation record from the University of California's Granite Mountains Desert Research Center (GMDRC), located at 1,311 m elevation, 50 km southwest of the York Fire footprint. Precipitation year is July 1 through June 30.**

**Figure 15. View northward from the base of Keystone Canyon in the eastern New York Mountains, taken in June 2023 prior to the York Fire. Approximately 40% of the California junipers were dead or dying as a result of the 2020-2022 drought, providing dry standing dead woody biomass as additional fuel for the York Fire, which would burn through the area a month later. Note also the prolific growth of native perennial grasses filling areas between trees and shrubs. Photo by J. M. André.**

Elimination of livestock grazing together with recurrent wildfires have the potential to return much of the area within the footprint of the York Fire to an ecological state more similar to what may have existed in pre-Euro-American settlement times. However, one part of the environmental equation has likely changed – the climate regime, particularly temperature. Episodes of high temperature and associated "hot drought" conditions exacerbate conditions conducive for the ignition and spread of wildfires. It is possible that the trajectory of climate change responsible for generating more intense, prolonged periods of heat may contribute to fire behavior that lies outside the range of variability of the area's historical wildfire regime. It seems clear, though, that the landscape contained within the footprint of the York Fire is conducive to wildfires even without the occurrence of non-native grasses as a fine fuel element. The amount of standing dry and flammable

biomass generated by the native perennial grass is more than adequate to carry a wildfire, particularly when vegetation is subjected to an increasingly prolonged, hot summer season with severe heatwaves, as predicted by climate change models. When extreme conditions of low humidity, high temperature, and wind co-occur, all that is required for extensive wildfire in such landscapes is an ignition source. Although the York Fire was human caused, the amount of fine fuel available in standing senescent or dormant perennial grasses makes wildfires inevitable in this landscape where lightning is the principal cause of ignition (*23*).

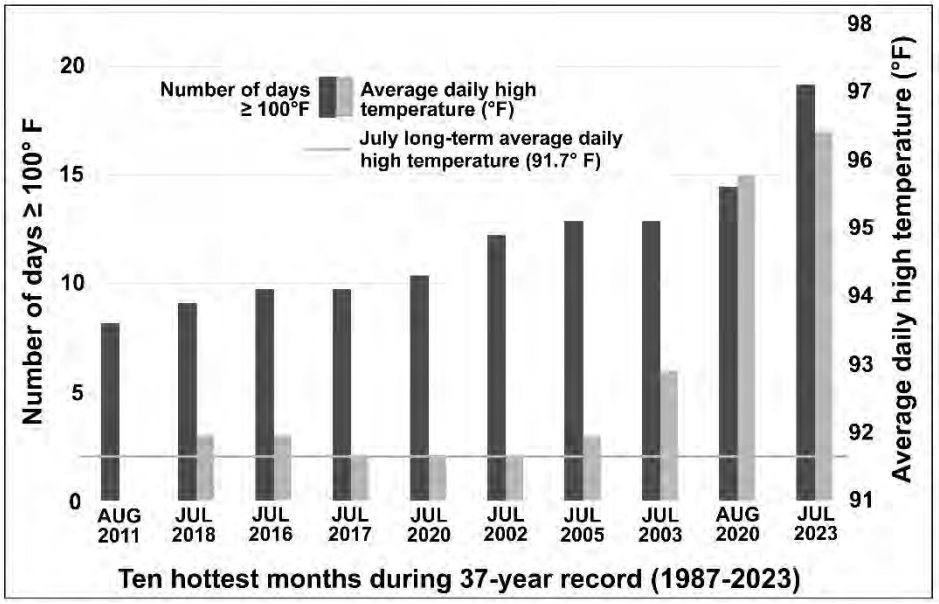


**Figure 16. Ten hottest months over the 37-year temperature record from the University of California's Granite Mountains Desert Research Center (GMDRC). Arranged left to right by total number of days reaching ≥ 100° F (dark bars) and showing the average monthly high temperatures for those months (gray bars), and the long-term average of July monthly high temperatures (gray horizontal line). The two most extreme records (August 2020, July 2023) represent conditions before and during the Dome Fire and York Fire, respectively. July 2023 exceeded most of the other hottest months by approximately 3° F.**

National Park Service policy states that "Every area with burnable vegetation must have an approved Fire Management Plan," and the first comprehensive plan for the Preserve to satisfy this mandate was completed 20 years ago, in 2004 (*48*). In that document, the occurrence of wildfires fueled by native grasses was recognized: "*Many of the higher elevation plant communities have a native perennial grass component that naturally occupies the spaces between shrubs, so the flammability of these communities is less influenced by the invasion of non-native grasses.*" (p. 17). Despite that recognition, the 2004 plan designated more than three-quarters of the land area within the Preserve for full wildfire suppression, including the entire area along the east side of the New York Mountains to Castle Peaks, all of Lanfair Valley, and the entirety of Cima Dome (Cima, Providence, and Lanfair Fire Management Units, pp. 31, 43, 51). Although National Park Service policy recognizes the value and potential use of fire as a management tool to restore vegetation, the landscape to the east side of the New York Mountains, including the northern portions of Lanfair Valley and Pinto Valley, contains scores of private inholdings that date to the homestead era. Many properties contain structures that are inhabited or used either permanently or seasonally. This patchwork of private inholdings presents an inconvenient reality in terms of policy and natural resource management due to the overwhelming demand for fire suppression in order to protect human life and property. This greatly restricts the potential for the use of fire, including natural ignitions by lightning, as a management tool.

The Fire Management Plan for the Preserve is currently in the process of being revised and updated (Debra Hughson, personal communication). Formulating policy regarding wildfire in the Preserve that effectively addresses multiple, and often conflicting needs and demands, such as those mentioned above, represents a significant challenge. However, knowledge of what kind of wildfire dynamics occurred long ago within parts of the Preserve serves as an essential foundation on which other considerations and needs can be addressed. An updated fire management plan also offers an opportunity to more accurately portray the nature and extent of vegetation dominated by perennial grasses in large parts of the Preserve, and the inherent and expected behavior of such vegetation with respect to wildfires. Information on the widespread occurrence and recurrence of pre-Euro-American settlement wildfires within what is now the footprint of the 2023 York Fire is an important contribution to the overall effort of developing a new, comprehensive Fire Management Plan.

*Acknowledgements*

Debra Hughson, Deputy Superintendent and Science Advisor of Mojave National Preserve has encouraged the investigation of fire history and helped secure financial support (Desert Southwest Cooperative Ecosystem Studies Unit Cooperative Agreement P21AC12169). The Desert Botanical Garden (DBG) financially supported initial ground survey work of JRM from 2017-19 and preliminary radiocarbon dating. Danilo Giordano (NPS) provided GIS shapefiles for wildfires, and James Aragon (BLM) provided the fire progression map for the York Fire. Aryn Musgrave, GIS Manager for the DBG prepared the fire footprint maps used in Figures 1 & 2. Greg Hodgins, former Director of the University of Arizona AMS radiocarbon dating laboratory, provided essential information on the application of wiggle-match radiocarbon dating, and Li Cheng of the laboratory provided advice on preparation of wood samples for radiocarbon dating. Laura Misajet of the Mojave Desert Heritage and Cultural Center provided access to archival

materials, including the oral history of Seth Alexander. Two anonymous reviewers and Tasha La Doux provided many helpful suggestions for improving the original manuscript and Carla McAuliffe assisted in the final editing and proofreading.

*References*


1. G. Tooley, "As Joshua trees burn, massive wildfire threatens to forever alter Mojave Desert," (Los Angeles Times, 1 August 2023); https://www.latimes.com/california/story/2023-08-01/mojave-desert-york-fire-containment-rain-joshua-trees-burning.
2. D. B. Taylor, "California's largest wildfire of the year sweeps across the Mojave," (New York Times, 1 August 2023); https://www.nytimes.com/2023/08/01/us/california-nevada-fire-york.html.
3. C. Thornton, "York wildfire still blazing, threatening Joshua trees in Mojave Desert," (USA Today, 2 August 2023); https://www.usatoday.com/story/news/nation/2023/08/02/california-york-fire-update/70511816007/.
4. N. Salahien, M. Gilbert, "Iconic Joshua trees burned by massive wildfire in Mojave Desert," (CNN News, 2 August 2023); https://www.cnn.com/2023/08/02/us/york-fire-california-nevada-wednesday/index.html.
5. E. Zerkel, "A plant that's everywhere is fueling a growing risk of wildfire disaster," (CNN News, 9 June 2024); https://www.cnn.com/2024/03/21/climate/wildfire-grass-risk-west-us/index.html.
6. J. McAuliffe, "Evidence for pre-settlement wildfires in perennial grass-dominated landscapes of the eastern Mojave Desert and implications for fire management in the Mojave National Preserve," (presentation at California Native Plant Society Conservation Conference, in Session 18: Fire and Native Plants, Los Angeles, California, 1-3 February 2018); https://milliontrees.me/wp-content/uploads/2018/02/cnps-conference-abstracts.pdf.
7. J. R. McAuliffe, Pre-Eurosettlement wildfires in Mojave National Preserve. Science Newsletter, 1-8 (2020); https://www.nps.gov/moja/learn/upload/2020_Science-Newsletter_w-alt-text-3_508.pdf.
8. J. R. McAuliffe, "Deciphering the record of pre-Eurosettlement wildfires, Mojave National Preserve, California," (Presentation delivered to BLM and NPS staff at Mojave National Preserve headquarters, Barstow, CA, 16 March 2020).
9. J. R. McAuliffe, "Establishing the history of pre-Eurosettlement wildfires using carbon-14 dating of fire-killed juniper trees in the Mojave National Preserve," (Desert Southwest Cooperative Ecosystem Studies Unit Cooperative Agreement P21AC12169, 2021-2024).
10. P. J. Reimer, et al., The IntCal20 Northern Hemisphere radiocarbon age calibration curve (0–55 cal kBP). *Radiocarbon*, **62**, 725-757 (2020).
11. C. Bronk-Ramsey, Radiocarbon dating: revolutions in understanding. *Archaeometry*, **50**, 249-275 (2008).
12. G. Hodgins, N. Kessler, M. Guebard, L. Hoedl, "An Introduction to Wiggle-Match Dating and an Examination of its Potential Impact on Chronological Studies in the Southwest" in *Pushing Boundaries in Southwestern Archaeology*, S. E. Nash, E. L. Baxter, Eds. (University Press of Colorado, 2023), pp. 116-133.
13. D. G. Casebier, "Interview with Seth Perry Alexander," *Bound transcription of original tape recording, Archives of Mojave Desert Heritage and Cultural Association, Goffs, California*, (176 p., 1978).
14. National Park System, Mojave Administrative History: Chapter two: Prelude to systematic federal management (2004); https://www.nps.gov/parkhistory/online_books/moja/adhi/adhi2.htm.
15. J. R. McAuliffe, Perennial grass-dominated plant communities of the eastern Mojave Desert region. *Desert Plants* **32**, 1-90 (2016); https://repository.arizona.edu/handle/10150/621587.
16. P. G. Rowlands, "Vegetational dynamics of the California Desert Conservation Area" in *The California Desert: An Introduction to Natural Resources and Man's Impact*, J. Latting and P.G. Rowlands, Eds. (June Latting Books, printed and bound by University of California, Riverside Press, 1995), pp. 185-211.
17. G. A. Foreman, Ed., *A Pathfinder in the Southwest – The Itinerary of Lieutenant A.W. Whipple During His Expedition for a Railway Route from Fort Smith to Los Angeles in the Years 1853 & 1854*. (University of Oklahoma Press, Norman, 1941).
18. B. J. Lefler, "Nuwuvi (Southern Paiute) Ecological Knowledge of Piñon-Juniper Woodlands: Implications for Conservation and Sustainable Resource Use in Two Southern Nevada Protected Areas," M.S. Thesis, Portland State University, Portland, Oregon (2014).
19. J.K. McAdoo, B.W. Schultz, S.R. Swanson, Aboriginal precedent for active management of sagebrush perennial grass communities in the Great Basin. *Rangeland Ecology and Management* **6**, 241-253 (2013).
20. S.G. Kitchen, Climate and human influences on historical fire regimes (AD 1400-1900) in the eastern Great Basin (USA). *The Holocene* **26**, 397-407 (2016).
21. C.C Black, Ecological implications of dividing plants into groups with distinct photosynthetic production capacities. *Advances in Ecological Research* **7**, 87-114 (1971).
22. S.S. Waller, J.K. Lewis, Occurrence of $C_3$ and $C_4$ photosynthetic pathways in North American grasses. *Rangeland Ecology & Management/Journal of Range Management Archives* **32**, 12-28. (1979).
23. M. L. Brooks, J.R. Matchett, Spatial and temporal patterns of wildfires in the Mojave Desert, 1980– 2004. *Journal of Arid Environments* **67**, 148-164 (2006).
24. K. L. Corbosiero, M.J. Dickinson, L.F. Bosart, The contribution of eastern north Pacific cyclones to the rainfall climatology of the southwest United States. *Monthly Weather Review* **137**, 2415-2435 (2009).
25. E.A. Ritchie, K.M. Wood, D.S. Gutzler, S.R. White, The influence of Eastern

Pacific tropical cyclone remnants on the southwestern United States. *Monthly Weather Review* **139**, 192-210 (2011).
26. W.H Romme, W.H., Allen, et al., Historical and modern disturbance regimes, stand structures, and landscape dynamics in piñon–juniper vegetation of the western United States. *Rangeland Ecology & Management* **62**, 203-222 (2009).
27. H. B. Johnson, "Vegetation and plant communities of southern California Deserts – A functional view," in *Plant Communities of Southern California, Special Publication No. 2*, J. Latting, Ed. (California Native Plant Society, 1976).
28. P.G. Rowlands, Vegetational attributes of the California Desert Conservation Area, in *The California Desert: An Introduction to Natural Resources and Man's Impact*, J. Latting and P.G. Rowlands, Eds. (June Latting Books, printed and bound by University of California, Riverside Press, 1995), pp. 135-183.
29. P. G. Rowlands, H. Johnson, E. Ritter, A. Endo, "The Mojave Desert" in *Reference Handbook on the Deserts of North America*, G.L. Bender, Ed. (Greenwood Press, Westport, Connecticut and London, England, 1982), pp. 103-162.
30. Thomas, K., T. Keeler-Wolf, J. Franklin, and P. Stine, "*Mojave Desert Ecosystem Program: Central Mojave Vegetation Database*," (U.S. Geological Survey Western Ecological Research Center & Southwest Biological Science Center. Sacramento, California, 2004).
31. K. A. Moloney, A. Fuentes-Ramirez, C. Holzapfel, Climate impacts on fire risk in desert shrublands: A modeling study. *Frontiers in Ecology and Evolution* **9**, (2021); https://doi.org/10.3389/fevo.2021.601877.
32. G. R. McPherson, "The role of fire in the desert grasslands" in: *The Desert Grassland*, M. P. McClaran and T.R. VanDevender, Eds. (Univ. of Arizona Press, Tucson, 1995), pp. 130-151.
33. S. R. Abella, K. S. Menard, T. A. Schetter, L. A. Sprow, J. R. Jaeger, J.F., Rapid and transient changes during 20 years of restoration management in savanna-woodland-prairie habitats threatened by woody plant encroachment. *Plant Ecology* **221**, 1201-1217 (2020).
34. B. R. Sturtevant, B. B. Hanberry, Processes underlying restoration of temperate savanna and woodland ecosystems: Emerging themes and challenges. *Forest Ecology and Management* **481**, (2021); https://doi.org/10.1016/j.foreco.2020.118681.
35. J.M Evens, K.G. Sikes, J.S. Ratchford, "Vegetation classification at Lake Mead National Recreation Area, Mojave National Preserve, Castle Mountains National Monument, and Death Valley National Park: Final report, (*Natural Resource Report NPS/MOJN/NRR—2020/2178*. National Park Service, Fort Collins, Colorado, 2020); https://doi.org/10.36967/nrr-2279201.
36. J.M Evens, K.G. Sikes, J.S. Ratchford, D. Stout, "Field Key to the Vegetation Alliances of Lake Mead National Recreation Area, Death Valley National Park, Mojave National Preserve, and Castle Mountains National Monument," (*California Native Plant Society Unpublished Report, submitted to USDI, National Park Service, Mojave Desert Network Inventory and Monitoring Program*. Sacramento, CA, 2020).
37. D. Cogan, "Vegetation mapping inventory project: Mojave National Preserve and Castle Mountains National Monument," (*Science Report NPS/SR—2024/225. National Park Service*, Fort Collins, Colorado, 2024); https://irma.nps.gov/DataStore/Reference/Profile/2306969.
38. E. Q. Margolis, Fire regime shift linked to increased forest density in a piñon–juniper savanna landscape. International *Journal of Wildland Fire* **23**, 234-245 (2014).
39. J. Aragon, "Description of observations during helicopter reconnaissance of York Fire front on second day of the York Fire," (*Recorded presentation on Zoom, Mojave Quarterly Community Meeting, Fire Management in Mojave National Preserve, April 4, 2024*).
40. M. L. Brooks, J. R. Machett, Plant community patterns in unburned and burned blackbrush (*Coleogyne ramossisima* Torr.) shrublands in the Mojave Desert. *Western North American Naturalist* **63**, 283-298 (2003).
41. K. J. Horn, J. Wilkinson, S. White, S. B. St. Clair, Desert wildfire impacts on plant community function. *Plant Ecology* **216**, 1623-1634 (2015).
42. K. J. Horn, S. B. St. Clair, Wildfire and exotic grass invasion alter plant productivity in response to climate variability in the Mojave Desert. *Landscape Ecology* **32**, 635- 646 (2017).
43. J. R. McAuliffe, Storm Cloud over Cima Dome – Tracking Vegetation Change after the Fire. *Science Newsletter*, 1-11 (2021); https://www.nps.gov/moja/learn/upload/2021MOJAscience-Newsletter-2021_508.pdf.
44. J.R. McAuliffe, E.P. Hamerlynck, Perennial plant mortality in the Sonoran and Mojave deserts in response to severe, multi-year drought. *Journal of Arid Environments*, **74**, 885-896 (2010).
45. K. E. King, et al., Increasing prevalence of hot drought across western North America since the 16th century. *Science Advances* **10**(4), (2024); https://www.science.org/doi/10.1126/sciadv.adj4289.
46. A. A. Gutierrez, et al., Wildfire response to changing daily temperature extremes in California's Sierra Nevada. *Science Advances*,**7**(47), (2021); https://www.science.org/doi/10.1126/sciadv.abe6417.
47. L. A. DeFalco, T. C. Esque, S. J. Scoles-Sciulla, J. Rodgers, J., Desert wildfire and severe drought diminish survivorship of the long-lived Joshua tree (*Yucca brevifolia*; Agavaceae). *American Journal of Botany* **97**, 243-250 (2010).
48. National Park Service, *Mojave National Preserve Fire Management Plan*, Barstow, California, USA, (2004); http://www.nps.gov/moja/parkmgmt/upload/fireplan.pdf.

# York Fire Authors' postscript 28 April 2025

Twenty months after the York Fire, native warm-season grasses – dormant, dry, and straw-colored – predominate across the landscape consumed in the fire. Without carefully examining the identities of those grasses, a casual observer passing through the area might interpret the scene as another example of post-wildfire "grassification" involving a tremendous increase and predominance of non-native grass species. However, this is not the case throughout the footprint of the York Fire. Precipitation from Tropical Storm Hilary in the third week of August 2023, combined with average winter precipitation of 2023-24 facilitated the resprouting and regrowth of native perennial grasses, including the predominant warm-season species (*Hilaria* spp., *Bouteloua eriopoda*, *Aristida purpurea*), as well as lesser amounts of native perennial cool-season species (*Stipa speciosa* and *Oryzopsis hymenoides*). Observations in mid-April 2025 (see photo) show the perennial grasses that have regrown are those that resprouted directly from the surviving, below-ground, root bases of established plants that were burned (above-ground) by the York Fire. Below-average warm-season precipitation in 2024 and the exceptionally dry winter-spring season of 2024-2025 impeded further growth and reproduction of those native grasses by either seedling establishment or the substantial lateral spread of existing plants (e.g., by rhizomatous tillering in the *Hilaria* spp. or stoloniferous reproduction in *B. eriopoda*). The extent of cover provided by native perennial grasses observed in April, 2025, is likely similar to, or no more than, that which was present before the fire. Notice that the non-native annual grass, red brome (*Bromus rubens*), is absent from the landscape in the photo. As discussed in the article, it was generally absent throughout the footprint of the York Fire; consequently, it likely remains absent or nearly so from the seed bank in this area. The widespread elimination or substantial reduction of Joshua trees and junipers by the fire greatly amplifies the visual dominance of the native perennial grasses and highlights their leading ecological role in the ecological dynamics of this entire landscape.

**View towards the northwest, approximately 1.7 km southwest of Barnwell in Mojave National Preserve (camera coordinates 35.28125°N, 115.25034°W). Photo by J. R. McAuliffe.**

The entire vista shown in the photo is within the footprint of the York Fire and non-native annual grasses are completely absent. Taken on 15 April 2025, the photo shows a landscape of dormant and dry native perennial grasses with scattered dead or severely impacted Joshua trees and junipers. All of the perennial grasses in this view are native plants that resprouted and grew from the surviving bases of individuals that were present before the fire. The small bunches in the foreground are *Hilaria jamesii*, together with scattered plants of *Bouteloua eriopoda*. Post-fire establishment of new plants from seed or asexual propagation has not yet occurred due to sparse warm-season precipitation during 2024 and the exceptionally dry conditions of the 2024-2025 cool season.

**The Mojave Science Newsletter highlights basic and applied academic research that contributes to a better understanding and wise management of California's expansive eastern Mojave Desert ecosystem. Particular emphasis is given to research conducted on, or relevant to, lands managed by the University of California, Mojave National Preserve, and adjacent public lands.**

The Mojave Science Newsletter is published by the Sweeney Granite Mountains Desert Research Center, University of California Natural Reserve System.

Editors: Tasha La Doux, James André, and Debra Hughson

Archived at:
https://granite.ucnrs.org/science-newsletter